TAMPEREEN TEKNILLINEN YLIOPISTO
TAMPERE UNIVERSITY OF TECHNOLOGY

JUHANI JOKINEN

PASSIVE INTERMODULATION IN HIGH-POWER RADIO TRANSCEIVERS

Master of Science Thesis

Examiner: Professor Mikko Valkama
The examiner and the topic were approved by the Council of the Faculty of Computing and Electrical Engineering on 9 December 2015

ABSTRACT

JUHANI JOKINEN: Passive Intermodulation in High-Power Radio Transceivers
Tampere University of Technology
Master of Science Thesis, 52 pages
March 2016
Master's Degree Program in Electrical Engineering
Major: RF Engineering
Examiner: Professor Mikko Valkama

Keywords: Passive Intermodulation, Nonlinear Distortion, RF, Digital Cancellation, Carrier Aggregation, Radio Transmitter

Passive intermodulation (PIM) is a phenomenon which occurs when at least two signals are fed into a nonlinear passive device or circuit. Sources for PIM can be divided into two groups, nonlinearities in metal junctions and nonlinear materials. The most common source for PIM is a loose or a bad metal connection. The problem is more in a base station side because PIM requires high powers and a base station can have high transmission (TX) power and receive (RX) power may be low. In addition, there are connectors in use at base stations and antennas with metallic junctions. Furthermore, a base station duplexer may have a high isolation between TX and RX port leading to a situation where intermodulation (IM) products due to TX power amplifier are attenuated well and PIM which is generated after the TX band-pass filter becomes significant. PIM is significant in the carrier aggregation technology, which uses more than one component carrier. In carrier aggregation, component carriers can be allocated non-contiguously on one or more frequency bands. If the duplex spacing is narrow, high-power 3^{rd} order PIM products may fall on RX frequency band and desensitize the transceiver's own receiver.

Digital IM cancellation is based on estimating how TX signals are modified at the path to the receiver by taking and processing samples of the received signal. Then the main idea is to regenerate replicas of IM products and subtract them from the received signal. The aim in this thesis is to demonstrate that PIM products, which are generated after the TX band-pass filter, can be reduced with digital cancellation. The duplexer that is used in measurements is a frequency band 1 base station duplexer which has 190 MHz duplex spacing. Because of that, lower than 7^{th} order IM products are not in the RX frequency band. For a reproducible test setup, a nonlinear connection at the antenna port of the duplexer is emulated with a diode.

The diode circuit generated high-power IM products already with +20 dBm TX power at the antenna port and with this power the TX filter completely attenuated the IM products due to the power amplifier. With the digital cancellation, the 7^{th} order IM product was successfully attenuated by 6 dB to 14 dB depending on the TX power. These measurement results demonstrate that it is possible to reduce PIM interference with digital cancellation. However, in this thesis the duplex spacing was considerably wide and therefore the most high-power 3^{rd} order IM products could not be measured. For future research it would be important to measure how digital cancellation works when the duplex spacing is narrow and PIM product power is higher but the order is lower.

TIIVISTELMÄ

JUHANI JOKINEN: Passiivinen intermodulaatio suuritehoisissa radiolähetin-vastaanottimissa
Tampereen teknillinen yliopisto
Diplomityö, 52 sivua
Maaliskuu 2016
Sähkötekniikan diplomi-insinöörin tutkinto-ohjelma
Pääaine: Suurtaajuustekniikka
Tarkastaja: professori Mikko Valkama

Avainsanat: passiivinen intermodulaatio, epälineaarinen särö, RF, digitaalinen kumoaminen, carrier aggregation, radiolähetin

Passiivinen intermodulaatio (PIM) on ilmiö, joka aiheutuu kun vähintään kaksi signaalia syötetään epälineaariseen passiiviseen laitteeseen tai piiriin. PIM lähteet voidaan jakaa kahteen ryhmään, epälineaarisiin metallikontakteihin sekä epälineaarisiin materiaaleihin. Yleisin PIM lähde on huonosti kytketty liitin. PIM on lähinnä tukiasema puolen ongelma, koska sen syntyminen vaatii suuren tehon ja tukiasemalla lähetys (TX) teho voi olla suuri ja vastaanotto (RX) teho saattaa olla pieni. Lisäksi tukiasemalla on käytössä liittimiä ja antennin rakenteessa on metalliliitoksia. Tämän lisäksi tukiaseman duplekserin TX ja RX portin isolaatio voi olla suuri, minkä vuoksi TX tehovahvistimen tuottamat intermodulaatio (IM) komponentit vaimentuvat hyvin ja TX kaistanpäästösuotimen jälkeen syntynyt PIM muuttuu merkittäväksi. PIM on merkittävä carrier aggregation tekniikassa, joka käyttää useampaa kantoaaltoa. Carrier aggregation mahdollistaa epäjatkuvan kantoaaltojen yhdistämisen yhdellä tai useammalla taajuuskaistalla. Jos dupleksointi väli on kapea, korkea tehoinen 3. kertaluvun PIM komponentti voi olla RX taajuudella ja häiritä lähetin-vastaanottimen omaa vastaanotinta.

Digitaalinen kumoaminen perustuu TX signaalien muokkaantumisen ja kytkeytymisen arviointiin, joka toteutetaan ottamalla ja prosessoimalla näytteitä vastaanotetusta signaalista. Perustana on generoida kopio IM häiriöstä ja vähentää se vastaanotetusta signaalista. Tavoitteena tässä opinnäytteessä on todentaa, että digitaalisella kumoamisella voidaan vähentää PIM häiriöitä, jotka ovat muodostuneet TX kaistanpäästösuotimen jälkeen. Duplekseri, jota käytettiin mittauksissa, on taajuuskaista 1:n tukiasema duplekseri, jolla on 190 MHz:n dupleksointi väli. Sen vuoksi alle 7. kertaluvun IM komponentit eivät ole RX taajuuskaistalla. Jotta testisysteemi olisi toistettavissa oleva, epälineaarista liitosta duplekserin antenni portissa on emuloitu diodilla.

Diodipiiri aiheutti korkeatehoisia IM komponentteja jo +20 dBm antenni portin TX teholla ja kyseisellä teholla TX suodin vaimensi kokonaan tehovahvistimen aiheuttamat IM häiriöt. Digitaalisella kumoamisella pystyttiin vaimentamaan 7. kertaluvun IM komponenttia 6 – 14 dB riippuen TX tehosta. Nämä mittaustulokset osoittavat, että PIM häiriöitä voidaan vähentää digitaalisella kumoamisella. Kuitenkin tässä opinnäytetyössä dupleksointi väli on merkittävän suuri, minkä vuoksi korkeampitehoista 3. kertaluvun IM komponenttia ei ollut mahdollista mitata. Tulevissa tutkimuksissa olisi tärkeää mitata kuinka hyvin digitaalinen kumoaminen toimii, kun dupleksointi väli on kapea ja PIM komponentin teho on korkeampi, mutta kertaluku on pienempi.

PREFACE

This thesis work has been done in Tampere University of Technology and I am grateful for Professor Mikko Valkama who provided this interesting topic and also supervised and advised me during this writing process.

I would like to thank you Adnan Kiayani who guided and helped me with the measurements done in this thesis. Furthermore, thank you Matias Turunen for the guidance in the circuit fabricating process. Also thank you Olli-Pekka Lundén for advising in the component selection and for the interesting lectures which are one of the reasons why I selected RF Engineering to my major. Also thanks for the interesting and fun discussions to Markus Allén with whom I shared the office room.

Finally the biggest thanks belong to my family and Mari Alitalo for supporting me during my studies. Especially thanks to Mari for the support in the end of my studies and during this thesis work process. Also thanks to all my friends with whom I shared unforgettable moments during my studies.

In Tampere, Finland, on 23 March 2016

Juhani Jokinen

CONTENTS

LIST OF FIGURES

LIST OF ABBREVIATIONS AND SYMBOLS

16-QAM	Quadrature Amplitude Modulation with constellation size of 16
3GPP	3rd Generation Partnership Project
4G	Fourth Generation
4-QAM	Quadrature Amplitude Modulation with constellation size of 4
64-QAM	Quadrature Amplitude Modulation with constellation size of 64
A/D	Analog to Digital
ANT	Antenna
CA	Carrier Aggregation
CC	Component Carrier
CC1	Component Carrier 1
CC2	Component Carrier 2
D/A	Digital to Analog
DUT	Device Under Test
E-UTRA	Evolved Universal Terrestrial Radio Access
FDD	Frequency Division Duplex
I/Q	In-phase Quadrature
IF	Intermediate Frequency
IM	Intermodulation
IM3-, IM5-, IM7-, IM9-	Negative Intermodulation product (3rd, 5th, 7th or 9th order)
IM3+, IM5+	Positive Intermodulation products (3rd or 5th order)
IMT-Advanced	International Mobile Telecommunications-Advanced
ITU	International Telecommunication Union
ITU-R	ITU Radiocommunication sector
LNA	Low-Noise Amplifier
LTE	Long Term Evolution
MIMO	Multiple Input Multiple Output
OFDMA	Orthogonal Frequency Division Multiple Access
OOB	Out-Of-Band
PA	Power Amplifier
PIM	Passive Intermodulation
QAM	Quadrature Amplitude Modulation
QPSK	Quadrature Phase Shift Keying
RB	Resource Block
RF	Radio Frequency
RX	Receive
SC-FDMA	Single Carrier – Frequency Division Multiple Access
TDD	Time Division Duplex
TX	Transmission

UE	User Equipment
VST	Vector Signal Transceiver

A_0	Amplitude
A_g	Generator amplitude
$a_0,\ a_1,\ a_2,\ a_3$	Taylor series coefficients
BW_1, BW_2	Bandwidths of original signals
BW_{IM}	Bandwidth of intermodulation product
$C_j(V)$	Nonlinear junction capacitance of diode
C_p	Diode's parasitic capacitance
f	Frequency
f_1, f_2	Frequencies of original signals
$f_{1,High}, f_{2,High}$	Signal 1 or 2 highest frequency
$f_{1,Low}, f_{2,Low}$	Signal 1 or 2 lowest frequency
f_{IM}	Frequency of intermodulation product
$f_{IM3,High}$	3rd order intermodulation product highest frequency
$f_{IM3,Low}$	3rd order intermodulation product lowest frequency
L_p	Diode's parasitic inductance
n, m	Integer coefficients
P_L	Power of the load
R_g	Generator series resistance
$R_j(V)$	Nonlinear junction resistance of diode
R_p	Diode's parasitic resistance
t	Time
V_d	Voltage of diode
$v_i(t)$	Input voltage
$v_o(t)$	Output voltage
$\omega_0, \omega_1, \omega_2$	Angular frequencies
x	Input
y	Output

1. INTRODUCTION

Data transmission in mobile devices is growing all the time because modern mobile phones can be used, for example, to Internet browsing and video streaming. Furthermore, it is possible to connect email accounts into the mobile phone and several applications may use data transmission, and consequently mobile phones are almost constantly using data transmission. The growing data usage in mobile devices and the growing number of devices demands higher data rates which require wider bandwidths and better flexibility in data transmission. International Mobile Telecommunications-Advanced (IMT-Advanced) standard has set requirements for peak data rates to 100 Mbit/s or 1 Gbit/s depending on the device mobility speed [1]. To achieve these data rates, new techniques have been developed and are further developed. These techniques are, for example, higher modulation techniques, multiple antenna usage and carrier aggregation (CA) [2].

The CA technique is based on aggregating more carriers for one user equipment (UE) which enables wider bandwidths for data transmission [2]. In the frequency division duplex (FDD) technique, the transmitting signal and the receiving signal uses different frequencies [3, p. 9]. In this type of transceiver, where transmitting and receiving are done simultaneously, CA may cause intermodulation (IM) problems. IM is generated when two or more signals with different frequencies are fed into a nonlinear system [4, p. 503]. If these signals have closely separated frequencies, IM products can be close to the original signals [4, p. 503]. In non-contiguous intra-band CA, component carriers (CCs) center frequencies are close to each other and the most high-power 3rd order IM product may be at receiver's frequency band if the duplex spacing is narrow. A significant source for IM is a power amplifier (PA) which is driven close to the saturation to achieve better power efficiency. These IM products due to a PA can be attenuated with a band-pass filter in the transceiver's duplexer. The duplexer isolates transmitted and received signals which both use the same antenna. Even though the IM products can be attenuated with the filter in the duplexer, the attenuation may not be enough when the received signal is significantly weaker [5, pp. 1-2]. Therefore, either the transmission (TX) power has to be lowered or the isolation in the duplexer increased by using filters with higher attenuation. However, both of these options have disadvantages because decreasing TX power decreases also the transceiver's coverage and increasing the attenuation will decrease the power efficiency and increase the filter's cost and complexity [3, p. 56]. One solution for this is a digital cancellation which is based on generating a replica of IM products and then subtracting it from the received signal. Some methods for digital IM cancellation are presented in studies [3] and [5]. However, those studies

are concentrated on the IM products generated in a nonlinear PA which is usually the most significant source of IM in a transceiver.

In a mobile UE the digital cancellation is important solution because it can reduce isolation requirements of the duplexer which decreases the size, cost and power consumption of the device. However, on a base station side the size and power consumption are not such problems as in mobile devices. Nevertheless, a base station transmitter may use much higher TX power than a mobile UE but still the received signals may have equal powers which require more isolation from the duplexer. The high TX power may also cause another problem known as passive intermodulation (PIM) [6]. The phenomenon is IM which is generated in nonlinear passive components or objects, like connectors, damaged cables or nonlinear materials. With powers high enough, a loosely connected connector, an antenna, ferromagnetic materials and also corroded materials may have a nonlinear response which causes PIM [6] [7]. These PIM products powers are lower than with IM products due to PA but the difference is that PIM can be generated between the duplexer and the antenna. Therefore, PIM products might be produced after the TX band-pass filter and in the worst scenario a high-power PIM product frequency is at receive (RX) band. This may lead to a situation where the desired RX signal is interfered or completely blocked by the PIM interference. Digital cancellation is useful also in this problem because it can be used to reduce PIM products which are generated after the duplexer TX filter. In conclusion, the digital cancellation is important in a mobile UE because it can reduce the size, cost and power consumption of the duplexer. In a base station the importance is that it can decrease the cost and mitigate PIM products which cannot be attenuated with the duplexer's filters.

In this thesis the focus is in the base station side where the duplexer isolation can be much higher than in mobile UE leading to the situation where PIM may become the most significant source of IM. With lower duplexer isolation or TX power the PIM may not be such a significant source compared to the IM due to the transceiver's PA. The scope of this thesis is to demonstrate that PIM products, which are generated after the TX filter as a cause of CA transmission in nonlinear components, can be reduced with digital IM cancellation. The measurement setup contains a base station PA and duplexer, and to achieve reproducible test, the PIM is generated with a diode. The diode is emulating a nonlinear connection between the duplexer and the antenna because diode's resistance depends on the current flowing through it.

The structure of this thesis is following. The second chapter introduces the harmonics and IM as phenomena in nonlinear systems and explains which are the frequencies and bandwidths of these products. Later in the same chapter PIM and common sources of it are explained, and also a comparison to the IM generated in active circuits is given. Finally in Chapter 2, a discussion is given about the issues caused by IM and how PIM can be tested. In the third chapter, the CA technique and some general requirements for unwanted emissions are presented. It is also explained why the non-contiguous intra-

band CA with narrow duplex spacing is more vulnerable for IM and how IM products can be prevented or digitally cancelled. In Chapter 4, the measurement setup is presented and it is also explained how PIM is emulated with a diode circuit between the duplexer and the antenna. The results of the measurements and discussion of them are given in the fifth chapter. In the sixth chapter, conclusions are given where the thesis topic and obtained results are summarized.

2. HARMONICS AND INTERMODULATION PRODUCTS

In a linear system or device, the output response is proportional to the input excitation in all cases [4, pp. 500-501]. A nonlinear system does not have exactly proportional output response with all input powers [4, pp. 500-501]. Semiconductors, like a diode, behave nonlinearly because diode's current is not directly proportional to the voltage, which is usual behavior for semiconductors. In addition, amplifiers behave nonlinearly because they contain semiconductors and they are limited by operating voltages which causes the saturation of the amplifier. Besides of active circuits containing semiconductors, also passive circuits may behave nonlinearly [6] [7]. These nonlinear circuits cause harmonics and also IM products. IM due to a nonlinear passive circuit is called PIM.

Harmonics are new frequency components which have integer multiple frequencies of the original signal frequency [4, p. 503]. When more than a single frequency component are present in the input, also IM products are generated which are sums and differences of the two original signals and harmonics [4, p. 503]. First in this chapter, generation of harmonics, IM and PIM are explained. Also discussion of avoiding PIM and comparison to IM due to active circuits are given. Finally in this chapter, issues due to IM and testing of PIM are introduced.

2.1 Harmonics in a Nonlinear System

To find out why harmonics are generated in a nonlinear system, it is needed to approximate the output response of the system. The output response can be estimated with Taylor series like in Equation (2.1) where y is the output and x is the input of the system at instant time, and a_0, a_1, a_2 and a_3 are Taylor coefficients [4, p. 501]. Only the first four terms of the approximation are introduced in Equation (2.1).

$$y_o = a_0 + a_1 x + a_2 x^2 + a_3 x^3 \ldots \tag{2.1}$$

Assume next that the input signal to the system is a sinusoid signal with amplitude A_0 and angular frequency ω_0. This input signal is shown in Equation (2.2) where $v_i(t)$ is the input voltage which is a function of time t.

$$v_i(t) = A_0 \cos(\omega_0 t) \tag{2.2}$$

By substituting Equation (2.2) to the output approximation, the output can be formed according to Equation (2.3). In this output approximation, only the first three terms from Taylor series are presented for simplicity.

$$v_o(t) = a_0 + a_1 A_0 \cos(\omega_0 t) + a_2 A_0^2 \cos^2(\omega_0 t) + \cdots \tag{2.3}$$

In Equation (2.3), the output $v_o(t)$ is voltage as a function of time. To expand the output approximation, trigonometric formula shown in Equation (2.4) can be adopted [8, p. 120].

$$\cos^2(a) = \frac{1}{2} + \frac{1}{2}\cos(2a) \tag{2.4}$$

The output of the system can be now expanded as in Equation (2.5) by adopting the trigonometric formula shown in Equation (2.4).

$$v_0(t) = a_0 + a_1 A_0 \cos(\omega_0 t) + \frac{1}{2} a_2 A_0^2 (1 + \cos(2\omega_0 t)) + \cdots \tag{2.5}$$

Now it is seen that there is a second harmonic in the output with angular frequency of $2\omega_0$. Also other harmonics can be solved from the Taylor series approximation by including more terms to the output approximation.

Harmonics can be typically filtered out easily from the output because they are multiples of the original frequency and therefore they are far from the desired signal frequency [4, pp. 503-504]. However, the situation usually is not this simple and it is more likely that multiple signals with different frequencies are fed in the input of the system.

2.2 Intermodulation

The output of the system becomes more complicated when two sinusoid signals with different frequencies are fed in the input. This kind of input signal can be like in Equation (2.6) if both signals have the same amplitude.

$$v_i(t) = A_0 \cos(\omega_1 t) + A_0 \cos(\omega_2 t) \tag{2.6}$$

Now the input signal consists of two signals with angular frequencies ω_1 and ω_2 and the amplitude is A_0 for both of the signals. Like in harmonics, Equation (2.6) can be substituted to the Taylors series approximation which gives Equation (2.7).

$$\begin{aligned} v_o(t) = a_0 &+ a_1 A_0 (cos(\omega_1 t) + \cos(\omega_2 t)) \\ &+ a_2 A_0^2 (cos(\omega_1 t) + \cos(\omega_2 t))^2 \\ &+ a_3 A_0^3 (cos(\omega_1 t) + \cos(\omega_2 t))^3 + \cdots \end{aligned} \tag{2.7}$$

In Equation (2.7), the first four terms from the Taylor series approximation are presented. To find out which frequency components will be in the output of the system, the approximation must be expanded. For this, the Binomial theorem and the trigonometric identities shown in Equations (2.8), (2.9), (2.10) and (2.11) can be adopted [8, p. 30;118;120].

$$(a+b)^2 = a^2 + 2ab + b^2 \tag{2.8}$$

$$(a+b)^3 = a^3 + b^3 + 3ab(a+b) \tag{2.9}$$

$$2\cos(a)\cos(b) = \cos(a-b) + \cos(a+b) \tag{2.10}$$

$$\cos^3(a) = \frac{3}{4}\cos(a) + \frac{1}{4}\cos(3a) \tag{2.11}$$

To expand the third and fourth term from Equation (2.7), Equations (2.8) and (2.9) are adopted, which forms Equation (2.12).

$$\begin{aligned} v_o(t) = a_0 &+ a_1A_0(cos(\omega_1 t) + \cos(\omega_2 t)) + a_2A_0^2(\cos^2(\omega_1 t) \\ &+ \cos^2(\omega_2 t) + 2\cos(\omega_1 t)\cos(\omega_2 t)) \\ &+ a_3A_0^3(\cos^3(\omega_1 t) + \cos^3(\omega_2 t) \\ &+ 3\cos(\omega_1 t)\cos(\omega_2 t)(\cos(\omega_1 t) + \cos(\omega_2 t))) + \cdots \end{aligned} \tag{2.12}$$

The cosine exponential functions can be expanded by adopting Equations (2.4) and (2.11). Also Equation (2.10) can be adopted to expand the cosine multiplications, which forms Equation (2.13).

$$\begin{aligned} v_o(t) = a_0 &+ a_1A_0(cos(\omega_1 t) + \cos(\omega_2 t)) \\ &+ a_2A_0^2\left(\frac{1}{2} + \frac{1}{2}\cos(2\omega_1 t) + \frac{1}{2} + \frac{1}{2}\cos(2\omega_2 t)\right. \\ &\left. + \cos(\omega_1 t - \omega_2 t) + \cos(\omega_1 t + \omega_2 t)\right) \\ &+ a_3A_0^3\left(\frac{3}{4}\cos(\omega_1 t) + \frac{1}{4}\cos(3\omega_1 t) + \frac{3}{4}\cos(\omega_2 t)\right. \\ &+ \frac{1}{4}\cos(3\omega_2 t) \\ &+ \frac{3}{2}(\cos(\omega_1 t - \omega_2 t) + \cos(\omega_1 t + \omega_2 t))(\cos(\omega_1 t) \\ &\left. + \cos(\omega_2 t))\right) + \cdots \end{aligned} \tag{2.13}$$

In Equation (2.13) the expanded third term of Taylor series shows that there are new components with angular frequencies $2\omega_1$, $2\omega_2$ and $\omega_1 \pm \omega_2$. These components are still very far away from the original signals if the original signals are relatively close to each other. From the expanded fourth term of Taylor series it can be already seen that

there are also new frequency components with angular frequencies $3\omega_1$ and $3\omega_2$ which also are far from the original frequencies and therefore easily to be filtered out. To find out which other new frequency components are generated in a nonlinear circuit, the last two factors of Equation (2.13) can be expanded by multiplying which is shown in Equation (2.14).

$$\begin{aligned}&\frac{3}{2}(\cos(\omega_1 t-\omega_2 t)+\cos(\omega_1 t+\omega_2 t))(\cos(\omega_1 t)+\cos(\omega_2 t)) \\ &=\frac{3}{2}(\cos(\omega_1 t-\omega_2 t)\cos(\omega_1 t) \\ &\qquad +\cos(\omega_1 t-\omega_2 t)\cos(\omega_2 t) \\ &\qquad +\cos(\omega_1 t+\omega_2 t)\cos(\omega_1 t) \\ &\qquad +\cos(\omega_1 t+\omega_2 t)\cos(\omega_2 t))\end{aligned} \tag{2.14}$$

The results of Equation (2.14) can still be expanded by adopting Equation (2.10) and also by knowing that $\cos(-x)=\cos(x)$ [8, p. 117]. This expanding is shown in Equation (2.15).

$$\begin{aligned}&\frac{3}{2}(\cos(\omega_1 t-\omega_2 t)\cos(\omega_1 t)+\cos(\omega_1 t-\omega_2 t)\cos(\omega_2 t) \\ &+\cos(\omega_1 t+\omega_2 t)\cos(\omega_1 t)+\cos(\omega_1 t+\omega_2 t)\cos(\omega_2 t)) \\ &=\frac{3}{2}\cos(\omega_1 t)+\frac{3}{2}\cos(\omega_2 t)+\frac{3}{4}\cos(2\omega_1 t-\omega_2 t) \\ &+\frac{3}{4}\cos(2\omega_2 t-\omega_1 t)+\frac{3}{4}\cos(2\omega_1 t+\omega_2 t)+\frac{3}{4}\cos(2\omega_2 t+\omega_1 t)\end{aligned} \tag{2.15}$$

From Equation (2.15) it is seen that there are new frequency components with angular frequencies of $2\omega_1 \pm \omega_2$ and $2\omega_2 \pm \omega_1$. In conclusion, when there are multiple signals present in the input of a nonlinear system, it causes several new frequency components to the output. These frequency components are integer multiples (harmonics) of the original signals, and also sum and difference frequencies of the original signals and harmonics [4, pp. 500-504]. Those sum and difference frequencies are called IM products and those frequency components may be very close to the original signals which can cause problems. IM products frequencies are the form of Equation (2.16) [4, p. 503].

$$f_{IM}=nf_1+mf_2 \tag{2.16}$$

Where f_{IM} is the frequency of the IM product, f_1 and f_2 are frequencies of original signals, and n and m are integer coefficients. The order of the IM product is the sum of the integer coefficients n and m [4, p. 503]. For example, $2\omega_1 \pm \omega_2$ is a 3rd order and $3\omega_1 \pm 2\omega_2$ is a 5th order IM product. These odd order IM products are close to the original signals if the original signals are relatively close to each other. To exemplify harmonics and IM products in frequency domain, an example output spectrum is shown in

Figure 2.1. As seen from Figure 2.1, only 3rd and 5th order products are close to the desired signals and other frequency components are relatively far. Frequency is represented with f in Figure 2.1.

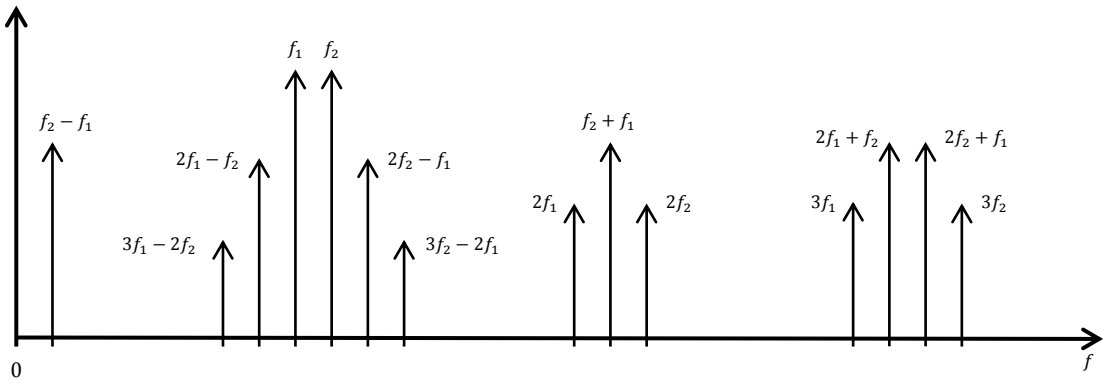

Figure 2.1 *Example output spectrum of a nonlinear device. The spectrum contains original signals f_1 and f_2. Also harmonics, and 3rd and 5th order IM products are presented in the spectrum.*

With modulated signals, the bandwidth of the IM product is wider than the original signals bandwidths and the higher the order of the product is the wider is the bandwidth [6]. If both original signals have the same bandwidth then the IM product bandwidth is the original signal bandwidth multiplied with the IM product order number [9]. But if the bandwidths of original signals are different, then the IM product bandwidth can be calculated with Equation (2.17).

$$BW_{IM} = |n|BW_1 + |m|BW_2 \tag{2.17}$$

In the equation, BW_{IM} is the bandwidth of IM product, BW_1 and BW_2 are the bandwidths of original signals, and n and m are the same integer coefficients used in Equation (2.16). Equation (2.17) can be explained with an example, where the first signal has 10 MHz bandwidth and the second signal has 20 MHz bandwidth. The first signal frequencies can be, for example, between $f_{1,Low} = 2100$ MHz and $f_{1,High} = 2110$ MHz and the second signal between $f_{2,Low} = 2150$ MHz and $f_{2,High} = 2170$ MHz. According to these, the 3rd order IM product frequency range can be calculated from these boundary frequencies of the original signals by adopting Equations (2.18) and (2.19).

$$f_{IM3,Low} = 2f_{1,Low} - f_{2,High} \tag{2.18}$$

$$f_{IM3,High} = 2f_{1,High} - f_{2,Low} \tag{2.19}$$

In these equations, $f_{IM3,Low}$ is the lowest and $f_{IM3,High}$ is the highest frequency of the 3rd order IM product. Equation (2.18) gives 2030 MHz for the low limit and Equation (2.19) gives 2070 MHz for the high limit with the example frequencies given. In conclusion, $f_{IM3,High} - f_{IM3,Low} = 40$ MHz is the bandwidth of the 3rd order IM product

which is $2BW_1 + BW_2$, which is the same form as Equation (2.17), with given example frequency values.

Furthermore, IM products may have very small amplitude with small input powers, but when the input power increases the IM products power increases more than the desired signals power [4, p. 504]. Increasing the desired signal output power by 1 dB will increase the 3rd order IM product power approximately by 3 dB and also other IM products will increase by the slope of the product order number [4, p. 504]. This phenomenon is seen from Equation (2.13) where the 3rd order signals amplitudes increases A_0^3 related to the input signal amplitude [4, p. 504]. This will lead to the situation where faster growing IM products may block out desired signals, when the input power is increased.

In conclusion, the IM happens in nonlinear systems which are for example nonlinear components and PAs. Semiconductors behave nonlinearly which makes them to be significant source of IM. PA contains semiconductors and it is also limited by the operational voltages, which is the reason that PA output response is nonlinear. The reason why PAs are operated near the saturation point is that the power efficiency is better. Reason for this is that the highest power efficiency for the PA can be achieved at the PA's saturation point [10, p. 524]. PAs are one major source of IM and because of that, it is important to design a PA to be as linear as possible.

2.3 Passive Intermodulation

Not only active components behave nonlinearly, but also passive circuits and components may have a nonlinear output response [4, p. 509] [6] [7]. If IM is generated due to a passive nonlinear circuit or component, the phenomenon is called PIM. PIM occurs at the same frequencies with IM products which are generated in active circuits, but usually PIM requires much higher powers to appear [11] [12]. This makes PIM more of a base station problem because at a base station high-power TX signals can be used and RX signals may have low power levels. Furthermore, the base station may contain several connectors and cables between different modules of the transceiver, which also make it vulnerable to PIM. This is because common PIM sources are connectors, damaged cables and antennas [7] [11]. Also old equipment, ferri- and ferromagnetic materials may generate PIM [6] [12]. Furthermore, PIM may be generated outside of the system like in corroded objects nearby the antenna [6] [7].

Sources of PIM can be divided into two groups which are the dominant reasons for the PIM [7]. First, the metallic contacts nonlinearity in connectors and antenna structures can behave nonlinearly [12]. This may be, because of not properly tightened connectors in transmission line or due to a damaged connector. Also contamination and oxidation in metallic contacts may generate PIM. The second group is nonlinear materials which are, for example, ferri- and ferromagnetic materials [12]. This is because of nonlinear

hysteresis effects in ferromagnetic materials, like iron or nickel and also some aluminum and copper alloys [6] [7]. Ferromagnetic materials are significant sources of PIM and their usage should be avoided in transceivers [6]. Ferrimagnetic materials may also generate PIM and transceivers might contain ferrimagnetic materials. For example, an isolator, phase shifter or circulator may be implemented with ferrimagnetic materials [4, p. 441] and if ferrimagnetic materials are used, they should be optimized for low PIM [6].

The source of PIM can also be outside of the system, for example, a corroded metal object nearby the antenna may generate PIM [6] [7]. This can happen if the transmission signal reaches the corroded object with high power. PIM is generated in corroded objects because of their semiconducting oxide layer on the metal [6]. This phenomenon is also known as Rusty Bolt Effect [6].

2.3.1 Passive Intermodulation in Metal to Metal Connections

Connectors are probably the biggest source of PIM [7] [11] and the reason for this nonlinear behavior in metal to metal connections, like in connectors, is that the connection is not perfect. There are always some very small gaps between two metal surfaces which can make the junction to be nonlinear at high powers or at a certain frequency. Furthermore, metal surfaces may have a very thin oxide layer and this layer and the air in the gaps form a thin insulator [6].

Because of the insulating layer between metal surfaces in the connection, the junction can have semiconductor like behavior [7]. This is because when the power increases in the conductor, the possibility for electron tunneling increases [13]. This phenomenon is also known as quantum tunneling and it means that electron may tunnel through a thin insulating layer with some probability [13]. The insulator between the metals forms a potential barrier and even if the electron does not have enough energy to go over this potential barrier, it may tunnel through it with some probability. Electron tunneling will increase the current in the junction and therefore decrease the resistance of the junction when the power increases. This electron tunneling is a significant reason for PIM, but usually it can happen only in very thin insulating layers [6] [14]. If the insulating layer is wider than 10 nm, the electron tunneling is not very potential to happen [6] [14]. Even when the layer thickness exceeds 2 nm, the possibility for electron tunneling drops significantly [15]. But if the junction is porous, for example, the corrosion has made porous oxide layer between metals, then the electron tunneling is possible even in thicker than 10 nm insulating layers [6].

Furthermore, the high power may also enable the Schottky effect where electrons have enough energy to exceed the potential barrier [6]. This Schottky effect also decreases the resistance of the junction as the power increases. Also, electric discharges may

cause PIM and also create new metallic contacts spots in the junction, which increases the conducting area [6].

Alternatively, if there is a high current density in the junction, it will heat the connector which will enlarge the existing gaps [6]. The connection may also be heated because of the sun light or other outside source [6]. These expanding gaps will lower the probability of tunneling, which increases the resistance of the junction. Also the temperature change itself changes the resistance, because the resistivity of the metals will change. Because of this, it is important to avoid high current densities [7].

In conclusion, in metal junctions there are always small gaps between two metal surfaces. This can cause nonlinearity to the junction and therefore generate PIM products. Contamination, abrasion and dust may lead to wider gaps which can make the insulating area of the connector to be thicker. Furthermore, dirt and possible metallic particles in the connector may cause nonlinear behavior [7]. All these reasons may cause PIM and therefore it is important that connectors are clean, properly tightened and not corroded. However, connectors are not the only source that generates PIM due to the electron tunneling and micro discharges. The other major source of PIM is the antenna of the transceiver [12] [13]. The antenna structure may also contain metal to metal junctions and it is also exposed to the environment temperature and humidity changes, which can lead to the corrosion. Therefore, the antenna may also generate PIM due to weak or corroded metallic contacts and it might even contain nonlinear materials [12]. Furthermore, there might be small cracks in the metallic structures, in which may also occur electron tunneling or small breakdowns [12].

2.3.2 Avoiding Passive Intermodulation

Because PIM may become a significant issue, especially at base stations, it is important to design the transceiver system to avoid PIM. First of all, any nonlinear materials, like ferromagnetic materials or carbon fiber, should not be used near the transmission lines or in the components which are used [7]. Also the current densities should be kept low to avoid heating and expanding of the metal junction gaps. Furthermore, the number of the connectors should be as low as possible, because they are the most common source of PIM, and also the cable lengths should be kept short [7].

Because the connectors are a big source of PIM, they should be designed for low PIM. Some connectors may contain ferromagnetic materials, like nickel or steel under the gold coating and they are definitely significant source of PIM [16]. Although, increasing the thickness of the gold plate will decrease the PIM, because the current density in ferromagnetic material decreases [16]. However, the PIM power level is related to the frequency, because the current density in the connector depends on the skin effect and with higher frequencies the current density increases on the connector surface. The PIM also depends on the connector size because with larger junction areas the current density

is lower. However, sometimes the size and the prize of the connector may determine, but there are connectors which are designed for low PIM. For example, DIN 7-16 connector is designed for low PIM and it has significantly lower PIM than SMA, BNC or N-connectors [6] [17]. The SMA-connector may have even 65 dB higher 3rd order PIM than with the DIN 7-16 connector when two signals of +43 dBm power is fed, this is shown in [17]. However, it is notable that this is only a result from a one research and it is relative to the used frequency, power and specific connectors. Although, it still demonstrates how a smaller SMA connector is more vulnerable to PIM than a large DIN 7-16 connector which is designed for low PIM.

Designing and using the low PIM components and connectors is not enough for avoiding the PIM products. A base station is exposed to the environment variables, contamination and corrosion. Therefore, it is important that the building and the maintaining of the base station are done properly. The connectors have to be tightened properly to avoid the PIM products, but overtightening may damage the connector and can possibly create metal particles inside the connector. Also the temperature variation may loosen the connectors, which makes the maintenance important. Furthermore, the connectors should be kept clean of dirt and corrosion. It is also important to pay attention into damaged cables and corroded objects at the antenna vicinity during the maintenances.

2.4 Differences between PIM and IM in Active Circuits

Although the phenomenon is the same in both, PIM and IM in active circuits, there are some differences. PIM requires higher powers but in active circuits, IM may appear even with low-power input signals, if the circuit is highly nonlinear. PIM may also be generated outside of the transceiver system when there is a corroded object nearby the high-power transmitting antenna [6].

In the transceiver, PIM may occur in different locations than IM generated in active circuits. To define this in more specifics, a simplified block diagram shown in Figure 2.2 is representing a part of a transceiver.

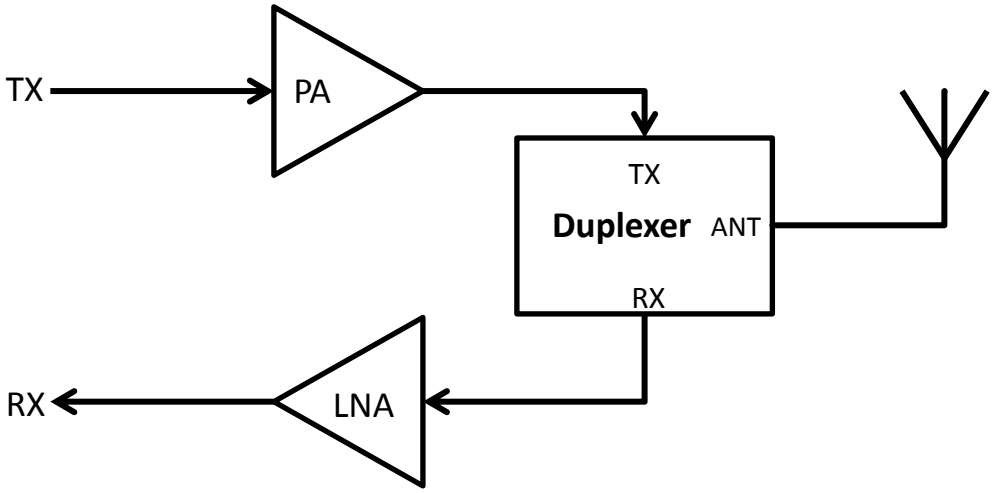

Figure 2.2 *Simplified transceiver block diagram which contain PA, duplexer, antenna and low-noise amplifier (LNA). The antenna port is marked as ANT.*

In Figure 2.2, there are only two amplifiers and a duplexer. The PA amplifies TX signal which goes to the duplexer. The duplexer has TX band-pass filter which in ideal case filters out completely all frequency components which are not in TX band. The filtered TX signal goes to the antenna port and is then transmitted. The RX signal comes from the same antenna and goes through the RX band-pass filter to the duplexer's RX port and then to the low-noise amplifier (LNA). In this simplified block diagram there are at least two possible active IM sources which are the nonlinear amplifiers, the PA and LNA. However, there are several possible sources of PIM depending on the physical implementation of the transceiver. The amplifiers and the duplexer may be different modules and connected to each other with cables and connectors. Also there are usually connectors between the duplexer and the antenna if the transceiver is a base station transceiver and not a mobile UE transceiver. Furthermore, the antenna itself is a possible source for PIM and also possible corroded objects nearby the antenna.

In conclusion, the source of PIM can be in several locations in the transceiver system and compared with IM due to active devices, PIM source may be also after the TX filter. Furthermore, IM due to active devices can be more predictable than the PIM sources, because PIM may be caused for several different reasons. It is also possible that the duplexer contains a circulator which is implemented with ferrimagnetic materials and therefore it can be a PIM source. However, the circulator may be active and use semiconductors instead of ferrimagnetic materials.

2.5 Issues Caused by the Intermodulation

IM is usually an unwanted phenomenon because it causes unwanted emissions which can be significantly close to the desired signals making them difficult to filter out [4, p. 504]. It is also possible that the IM products are at the operating RX band of the transceiver system. Because of the finite isolation of the duplexer, the IM products may leak

into the RX chain of the transceiver [3, p. 56]. To define the issue in more specifics, an example of a base station transceiver's spectrum is shown in Figure 2.3 which contains two CCs, and 3rd and 5th order IM products which are marked as IM3-, IM3+, IM5- and IM5+. Furthermore, the duplexer's band-pass filters stop-band attenuation is demonstrated in the figure.

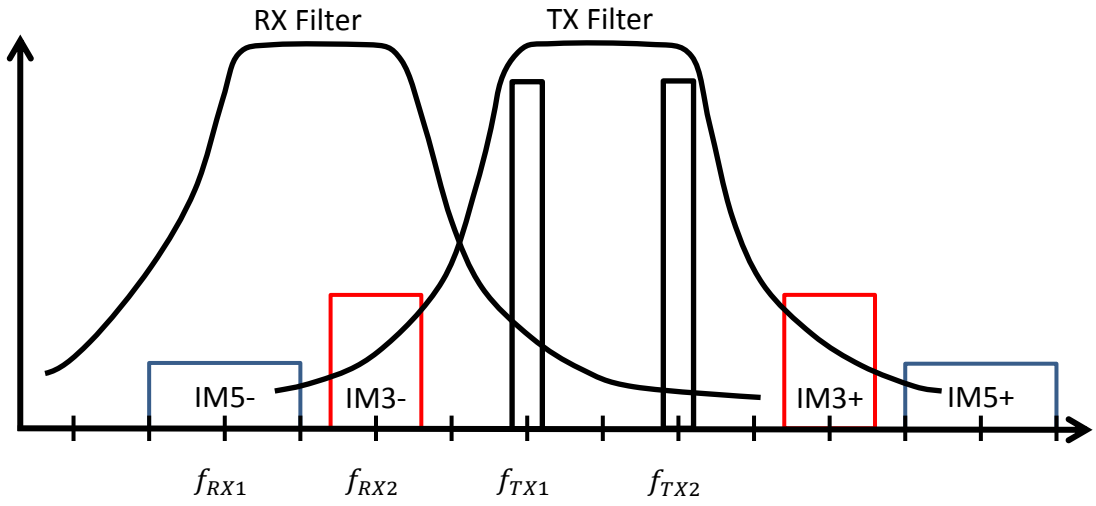

Figure 2.3 *Example of transceiver's spectrum where black rectangles represents TX signals, red represents 3rd order IM products and blue 5th order IM products. The filter curves represent the stop-band attenuation.*

As seen from Figure 2.3, the filters' stop-band attenuations are not ideal and therefore IM products may leak to the RX chain of the transceiver. In the worst case, the IM product frequency is directly at the transceiver's own RX operating frequency. Because the desired RX signals may be considerably weaker than the IM products, the IM interference may block completely the desired RX signal [5, pp. 1-2]. However, this is a problem only in a FDD technique where the transmitting and receiving are done simultaneously.

The IM products may not only cause disruption to the transceiver's own receiver, but also to the other receivers if the IM products are transmitted [6]. Especially in a situation, where a transmitting antenna and another receiver antenna are close to each other. Even though the IM product may have significantly low power, it can still raise the noise floor, because higher order products have wide bandwidths [6].

In conclusion, even that the TX filter can attenuate remarkably unwanted emission it is still possible that PIM products are transmitted to other receivers or leaked into the RX chain. This is because PIM may be generated after the TX filter, for example in the antenna structure or in the connectors between the duplexer and the antenna. Furthermore, old equipment may also start causing PIM because they may not be designed for new frequencies which might be taken into use.

2.6 Testing of the Passive Intermodulation

To test PIM, it is needed to generate the PIM products with two test signals, whose frequencies are closely spaced. The PIM testing can be divided into two groups, radiating and non-radiating measurements [7]. In radiating testing, the TX signals are sent from an antenna to the device under test (DUT) and the signals are received with another antenna. The PIM products are then filtered from the RX signals [7]. The radiating testing can be used, for example, for testing an antenna in an anechoic chamber, but the control of the environmental parameters might be difficult [7].

The non-radiating testing can be done with reverse or forward testing [6]. In reverse testing, two signals are transmitted into the DUT through the duplexer and the reflected PIM products are measured from the RX port of the duplexer [6] [7]. This measurement can be done only for the DUT or for the whole transceiver system with several possible sources of PIM. However, measurements with two fixed frequency test signals may not give accurate results, because depending on the electrical lengths of the cables, the reflected signals may add or cancel other signals [6]. Therefore, this type of measurement should be done with one fixed frequency and with one sweeping frequency. Another possibility is to do this measurement two times where the second measurement uses different frequency with the other test signal and then results can be compared. In Figure 2.4 is the block diagram of the reverse PIM testing for the DUT.

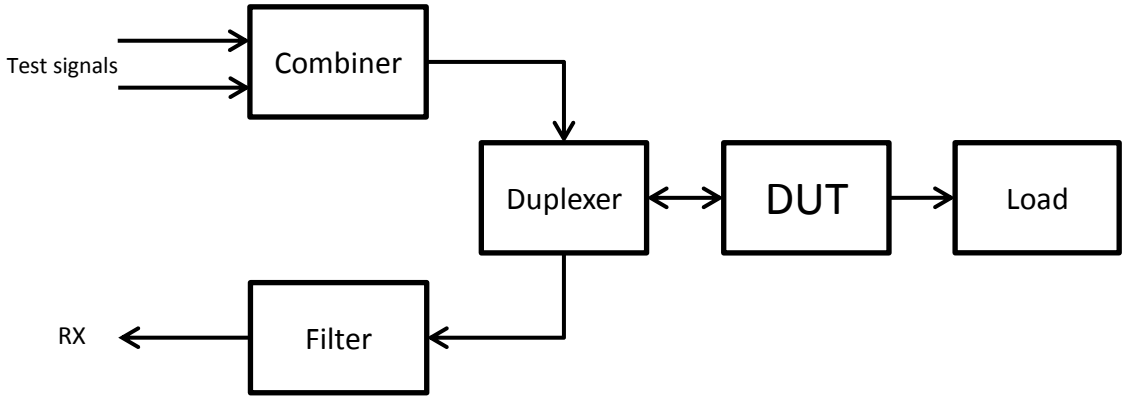

Figure 2.4 *The test signals have closely separated frequencies and reflected PIM products generated in DUT is measured from the duplexer's RX port. The filter is used to filter out the test signals.*

The components used in the PIM measurement should be as linear as possible to achieve low IM generation in measurement devices. The load is also one possible source for PIM and it should be as linear as possible [7]. To get more accurate results, the system should be measured first without the DUT to get the residual IM power level of the test system [6].

The forward testing can be done with examining the output of the DUT or transceiver system. Similar to the reverse measurement, two test signals are fed into the DUT or to

the system. After the DUT, the PIM products are filtered and measured from the output. The PIM products can be extracted from the output signal with a coupler and filter [6] [7]. A block diagram of forward PIM testing for DUT is shown in Figure 2.5.

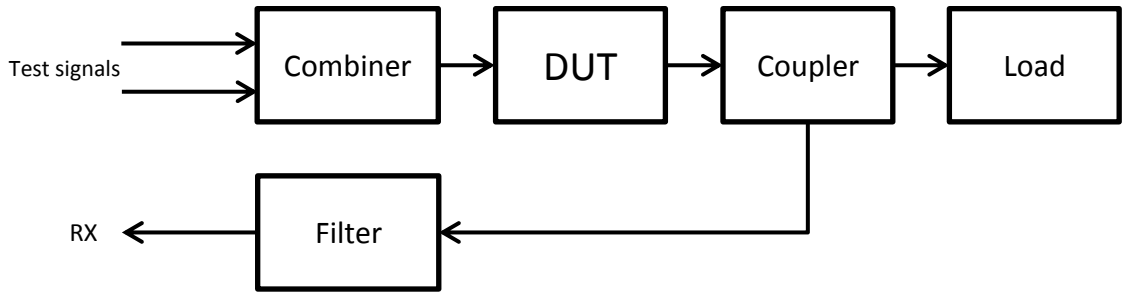

Figure 2.5 *Like in the reverse testing, the test signals are fed into the system and PIM generated in DUT is measured. In Forward testing PIM is measured after the DUT with a coupler and filter.*

As in the reverse testing, the measurement equipment should be designed for low PIM and now the coupler is also a possible source to generate PIM [7]. With the forward testing it is also possible to measure an antenna, but instead of the coupler and load, there is another antenna for receiving the PIM products. However, the forward testing is not as common as reverse testing [6].

In general, it is needed to make sure that the measurement instrument, which examines the PIM signals, is not in saturation. If the measuring instrument is saturated, it may generate also IM and due to that the results are not correct [18, p. 371]. Fortunately it is easy to verify that the measuring equipment is not generating IM, by adding an attenuator into the input port of the instrument. If the power levels of the IM products decrease as much as the added attenuation was, then the instrument was not generating IM products. However, if the power levels of the IM products dropped more than the value of added attenuation, then the instrument was in saturation. Attenuation needs to be added until the decrease of power levels is the same as the value of added attenuation [18, p. 371].

As discussed in Section 2.3 the system has to use high-power TX signals to generate PIM products. Currently there are no specific power levels defined, which have to be used in PIM testing in a cellular system [6]. Also there are no specific limits for generated PIM level, because it depends on the used powers in test signals. The only specification related to PIM is IEC 62037 standard which is developed for the component manufacturers to enable the comparison of linearity between different devices [6]. The IEC 62037 standard was published in 1999 and it is replaced with new standard series which are published in 2012 and 2013 [19]. The IEC 62037 standard recommends that the power of test signals should be +43 dBm (20 W), which is the power that many manufacturers have been using in PIM testing [6] [20]. However, this standard is only for comparing components and it does not specify any limits for PIM, but The Interna-

tional Electrotechnical Commission is developing a new standard for PIM limits [20]. This task is assigned for Technical Committee 46 Working Group 6 (TC 46/WG 6) [21].

However, even though there are not exact limit specifications for PIM in single components, there are specifications for unwanted emissions in wireless communication. These specifications define the power density limits for unwanted emissions at UE and base station transceivers. These specifications categorize unwanted emissions into three groups which are in-band emissions, out-of-band (OOB) emissions and spurious emissions [22]. In-band emissions are emissions at the TX operating frequency band. OOB emissions frequency range starts from the edges of the operating TX frequency band. Finally, the spurious emissions are emissions outside of the OOB and in-band region [23, p. 121]. These unwanted emissions maximum power density limits are specified depending on the used transmission technique, operating frequency band and bandwidth. In Section 3.3, some of the general unwanted emission limits for a base station transmitter are introduced.

3. CARRIER AGGREGATION AND INTERMODULATION DISTORTION CANCELLATION

Mobile data transmission has been growing rapidly in the past years because the number of wireless devices has been growing. Modern mobile devices also enable, for example, the using of Internet and video streaming. Furthermore, different applications in wireless devices are using data transmission and it is more likely that the UE is almost constantly connected to the cellular network. In addition, video streaming, for example, requires significantly wide transmission bandwidth which also sets up challenges for the cellular network. First solution for this rapidly increasing data transmission was Long Term Evolution (LTE) which was introduced in 3rd Generation Partnership Project (3GPP) Releases 8 and 9 [24, p. 1]. However, the LTE technique does not fulfill the data rates which are required in fourth generation (4G) devices. Therefore, LTE-Advanced was introduced in 3GPP Release 10 to fulfill even higher data rate requirements and to enable wider bandwidths in wireless data transmission [24, pp. 1-10]. However, the CA technology, which is used in LTE-Advanced, can cause IM problems.

In this chapter, an overview of the LTE technology is introduced first, continuing to the LTE-Advanced and CA technology. After that, some of the general limits for unwanted emissions at a base station are introduced. Finally in this chapter, the IM products mitigation techniques are introduces. The mitigation techniques are separated to the duplexer isolation and digital IM cancellation.

3.1 Long Term Evolution

LTE is a technology which was designed to give users higher data rates and quality in the cellular network. LTE technology uses orthogonal frequency division multiple access (OFDMA) technique in a downlink which is the data connection from a base station to an UE [24, p. 14]. In the uplink, LTE technology uses single carrier – frequency division multiple access (SC-FDMA) technique which does not require as linear PA as the OFDMA technique requires [25].

In LTE OFDMA modulation, the signal consists of orthogonal subcarriers which are separated closely to each other and every subcarrier has been modulated with different data symbols [3, p. 9]. SC-FDMA is very similar to OFDMA, but the data is spread to the all subcarriers instead of modulating all subcarriers with a different data symbol [3, p. 12]. The spacing of the subcarriers is 15 kHz and 12 subcarriers forms one resource block (RB) which bandwidth is 180 kHz [24, p. 15]. Number of RBs demands the chan-

nel bandwidth which can be 1.4 MHz, 3 MHz, 5 MHz, 10 MHz, 15 MHz or 20 MHz [26, p. 38]. These bandwidths were specified first in 3GPP Release 8. The relation between subcarriers and the channel bandwidth is shown in Table 3.1 [24, p. 16].

Table 3.1 *Possible channel bandwidths in LTE, and number of subcarriers and RBs with different bandwidths.*

Bandwidth (MHz)	1.4	3.0	5	10	15	20
Subcarriers	72	180	300	600	900	1200
Resource Blocks	6	15	25	50	75	100

In LTE, data in subcarriers are modulated with Quadrature Phase Shift Keying (QPSK) or with Quadrature Amplitude Modulation (QAM) [26, p. 41]. In both modulations, the phase is modulated and in QAM also the amplitude is modulated. In both modulations, the data consists of two signals which have 90° phase shift between them, which forms a complex-value signal [3, pp. 13-14]. The real part of the complex valued signal is called the in-phase signal and the imaginary part is the quadrature signal [3, p. 14]. Possibilities in QAM are 16-QAM or 64-QAM in LTE, which means that the constellation size can be 16 or 64 points. QPSK is the same as 4-QAM, in other words QPSK has the constellation size of 4 points. Different modulation constellation points are shown in Figure 3.1.

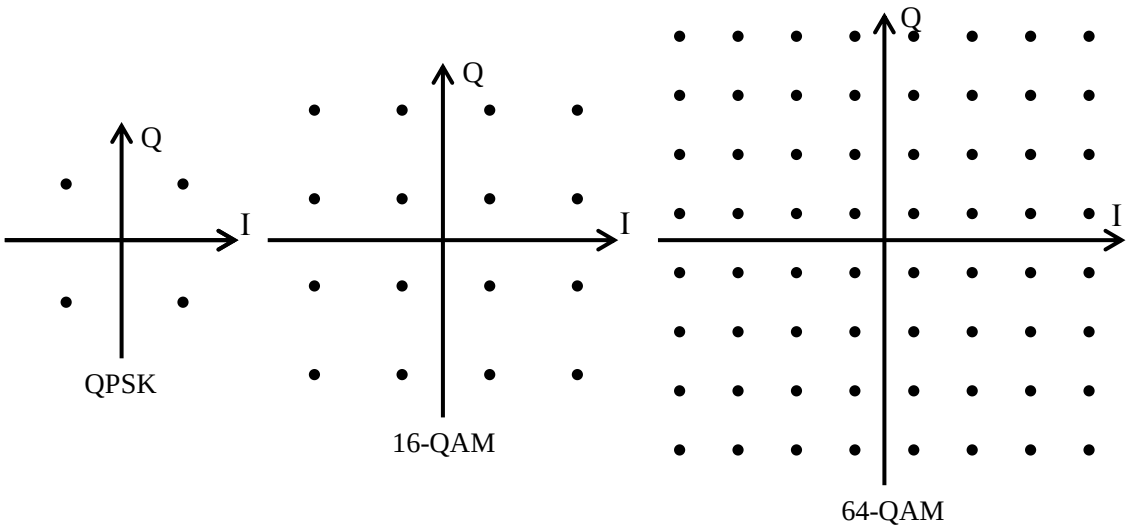

Figure 3.1 *Different data points in possible modulations of LTE. QPSK has 4 different data points which makes it equal to 4-QAM modulation.*

The modulation type depends on the signal strength between the base station and the UE. If the signal strength is weak, constellation point count has to be low because otherwise the data may become distorted. As seen from Figure 3.1, increasing the constellation size the distance between data points decreases, which increases the possibility of misinterpretation if the received signal is distorted enough. Furthermore, it is possible to use spatial multiplexing up to 4x4 multiple input multiple output (MIMO) technique

[25]. In spatial multiplexing the data stream is split into smaller data streams which are transmitted with different antennas at the same time and also received with multiple antennas, which increases the data rate [24, p. 21]. In 4x4 MIMO there are 4 antennas transmitting and 4 antennas receiving the split data stream.

Theoretical maximum peak data rates in LTE are 300 Mbps in the downlink and 75 Mbps in the uplink [24, p. 28] [25]. To achieve these data rates, the channel bandwidth has to be 20 MHz and the signal strength should be strong enough to enable the use of 64-QAM modulation, and also 4x4 MIMO has to be used [24, p. 28]. However, these maximum data rates are only theoretical values and still do not fulfill 4G requirements for peak data rates which is one reason for developing LTE-Advanced.

3.2 Carrier Aggregation in LTE-Advanced

The International Telecommunication Union (ITU) has the ITU Radiocommunication Sector (ITU-R) which has defined the IMT-Advanced standard. This IMT-Advanced standard is also referred to as 4G whose requirement for the peak data rate is 1 Gbps [1]. This requirement relates to the low mobility case where the UE is at a fixed position or moves slowly related to the base station. For high mobility case, where the UE moves fast, the requirement is 100 Mbps [1]. Because the LTE technology from 3GPP Releases 8 and 9 did not fulfill IMT-Advanced requirements, LTE-Advanced was developed and first introduced in Release 10. The theoretical maximum peak data rate for LTE-Advanced is 3 Gbps in the downlink side and 1.5 Gbps in the uplink side, which measures up to the IMT-Advanced requirements [2]. 3GPP is still developing LTE-Advanced and CA is one of the new functionalities in it. The main idea in CA is to increase bandwidth by aggregating more carriers for a single UE.

Because it is needed that older UEs (Release 8 and 9 UEs) are compatibles to the cellular network, CA is based on 3GPP Release 8 and 9 carriers which are referred to as CCs in LTE-Advanced [2] [27, p. 86]. This makes it possible that Release 8 and 9 UEs can use the same cellular network with Release 10 and onwards UEs. LTE-Advanced UE can use more than one CC at the same time and this is the main idea in CA. The maximum limit for CCs in CA is specified to 5 which increases the maximum bandwidth to 100 MHz, because the maximum bandwidth for one CC is 20 MHz [2] [27, p. 86] [28, p. 12]. Aggregated CCs do not have to have the same bandwidth and also the number of CCs in the uplink and downlink does not have to be the same [2]. Although, in the uplink the CC count has to be equal to or lower than the number of CCs in the downlink [2] [29]. However, 3GPP has been proposed that it would be reasonable to limit the amount of different bandwidths in CA to two [30, p. 14]. This would mean that it is not allowed to use, for example, bandwidths 5 MHz, 15 MHz and 20 MHz in three CCs to reach 40 MHz aggregated bandwidth [30, p. 14]. Instead of this, the aggregated bandwidth should be formed, for example, with two 10 MHz CCs and one 20 MHz CC. This leads to the same aggregated bandwidth by using only two different CC bandwidths.

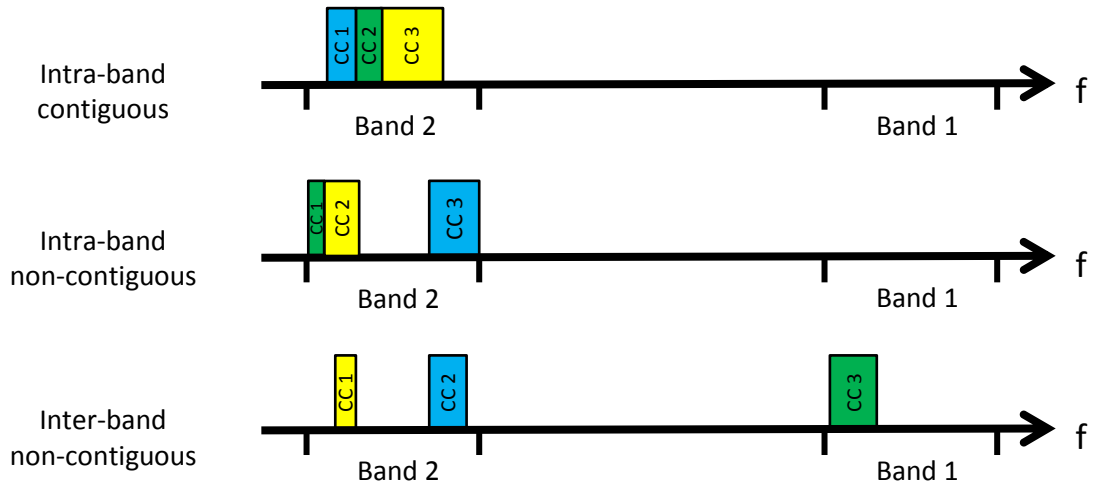

Figure 3.2 *An illustration of different aggregation possibilities in CA, where all CCs have different bandwidths.*

In the CA technology, CCs can be aggregated in three different ways as seen from Figure 3.2. The frequency bands seen in Figure 3.2 are frequency bands used in LTE which are referred to evolved universal terrestrial access network (E-UTRA) bands. The first possibility is intra-band contiguous aggregation where all CCs are aggregated contiguously to the same E-UTRA band. This contiguous aggregation type is simple but often it might be difficult to provide over 20 MHz contiguous bandwidths for single UE at the same frequency band [2]. The second possibility is that all CCs are at the same E-UTRA band, but they are aggregated non-contiguously. This intra-band non-contiguous aggregation gives more flexibility to the spectrum and makes it easier to arrange wide bandwidths for a single UE [2]. The last possibility is that all CCs are not in the same E-UTRA band and also they might be aggregated non-contiguously if some of them are at the same E-UTRA band. This inter-band non-contiguous aggregation gives even more flexibility to the spectrum and it increases the possibility to achieve wider bandwidths for single UE.

LTE CA can be used in FDD or in time division duplex (TDD) technologies [29]. In FDD the uplink and downlink uses different carrier frequencies, and the transceiver transmits and receives at the same time. The TDD transceiver either transmits or receives, and both uplink and downlink uses the same carrier frequency. In this thesis, the scope is on FDD transceivers, because they are vulnerable to the own RX desensitization due to simultaneous transmitting and receiving.

All CC combinations are not possible, because E-UTRA band and CC count combinations are specified in 3GPP Releases 10 and onwards [2]. The CA CC combinations are specified by 3GPP to avoid complexity [27, p. 86]. Specific aggregation combinations also define the maximum aggregated bandwidth. In Release 10, only three CA CC combinations were defined which were intra-band contiguous in FDD and TDD, and one inter-band FDD combination [29]. In Release 11, several new CA combinations and

also intra-band non-contiguous combination were defined [29]. All introduced CA combinations in Releases 10 and 11 had only two CCs and the maximum aggregated bandwidth was 40 MHz [29]. In later 3GPP Releases (12 and beyond) several CA CC combinations have been introduced and also combinations which contain more than two CCs, and enable wider than 40 MHz aggregated bandwidths [28] [31].

3.3 Unwanted Emissions Power Density Limits in LTE and LTE-Advanced

Unwanted emission can be divided into OOB emissions and spurious emissions [32, p. 36]. Requirements for these unwanted emissions at a base station transceiver are specified by 3GPP in [32]. In this section, some of these general requirements for a base station are introduced to give understanding about allowed power density levels. In OOB domain, the requirements for the base station transmitter are specified by Adjacent Channel Leakage Ratio and operating band unwanted emission limits [32, p. 36]. Outside the OOB domain, the power limits are specified by the spurious emissions limits [32, p. 36] which are more relevant in the scope of this thesis.

In the spurious emissions domain, which starts from OOB domains edges, the spurious emissions limits are not allowed to be exceeded [32, p. 36]. The base station transmitter spurious emissions domain is from 9 kHz to 12.75 GHz but excluding the domain which starts from 10 MHz below the operating downlink band and ends to 10 MHz above the operating donwlink band [32, p. 55]. For example, in E-UTRA band 1 the spurious emissions domain is from 9 kHz to 12.75 GHz but excluding frequencies from 2100 MHz to 2180 MHz, because the downlink band is from 2110 MHz to 2170 MHz. The general spurious emissions limits for Category A and Category B base stations are shown in Table 3.2 [32, pp. 55-56]. Category A base station limits are not specified for any region and it has more relaxed limits than Category B, C and D which are specified for different regions [33, p. 7]. Category B power limits are specified and adopted in Europe [33, p. 7].

Table 3.2 *Base station spurious emissions maximum power level limits for Category A and B base stations.*

Frequency range	Maximum power Category A (dBm)	Maximum power Category B (dBm)	Measurement bandwidth
9 kHz – 150 kHz	-13	-36	1 kHz
150 kHz – 30 MHz	-13	-36	10 kHz
30 MHz – 1 GHz	-13	-36	100 kHz
1 GHz – 12.75 GHz	-13	-30	1 MHz

In conclusion, transceiver's emissions cannot exceed power density limits which are specified by 3GPP. These limits depend on the used transmission technique, operating

frequency and channel bandwidth. There might be also additional requirements for some specific E-UTRA bands and geographical locations.

3.4 Intermodulation in Carrier Aggregation

In CA TDD technique, the leakage of transceiver's own TX IM products to the own receiver is not a problem because the transmitting and receiving are not done simultaneously. In FDD technique, the problem is obvious because the transmitting and receiving are done at the same time. Especially in FDD with intra-band non-contiguous CA, the problem is significant because there are at least two CCs separated by a relatively narrow frequency gap, which causes the IM close to the CCs. In this type of non-contiguous CA, it is possible that the IM products fall on the RX band, which can cause receiver desensitization [5]. The problem is in both, intra-band and inter-band non-contiguous aggregation, but in this thesis the focus is in intra-band case.

The duplex spacing defines the frequency gap between TX and RX operating frequency. Each E-UTRA band has been defined in 3GPP releases and the duplex spacing can be calculated from TX and RX band frequencies difference. For example, band 1 has the duplex spacing of 190 MHz, but band 2 duplex spacing is only 80 MHz which is significantly narrow [23, p. 56] [34, p. 11]. Both bands 1 and 2 still have the same bandwidth which is 60 MHz. E-UTRA bands 1 and 2 frequencies, duplex spacing and frequency bandwidth are shown in Table 3.3 [34, p. 11].

Table 3.3 *E-UTRA band 1 and 2 specifications. Frequency bands are close to each other and the bandwidths are the same but the duplex spacing of band 1 is 110 MHz wider than the duplex spacing of band 2.*

E-UTRA Band	Downlink frequency (MHz)	Uplink frequency (MHz)	Duplex spacing (MHz)	Bandwidth (MHz)
Band 1	2110 – 2170	1920 – 1980	190	60
Band 2	1930 – 1990	1850 – 1910	80	60

In Table 3.3, the frequencies are named as downlink and uplink frequencies. A narrow duplex spacing leads to bigger problems in intra-band non-contiguous CA, because the frequency gap between CCs defines the frequencies of IM products. If this gap is almost as wide as the duplex spacing, then even 3^{rd} and 5^{th} order products can be at the transceiver's own RX frequency. If the duplex spacing is much wider than the gap between the CCs, then there can still be 7^{th} and 9^{th} order IM products at RX frequency band. Furthermore, if the CCs have wide bandwidths, then the IM products have significantly wide bandwidths leading to the situation where several IM products may fall on RX frequency band. Illustration of the IM products at E-UTRA band 2 is shown in Figure 3.3. It is important to notice that Figure 3.3 is only a simple illustrative example and the form of an IM product is not an ideal rectangular in the spectrum.

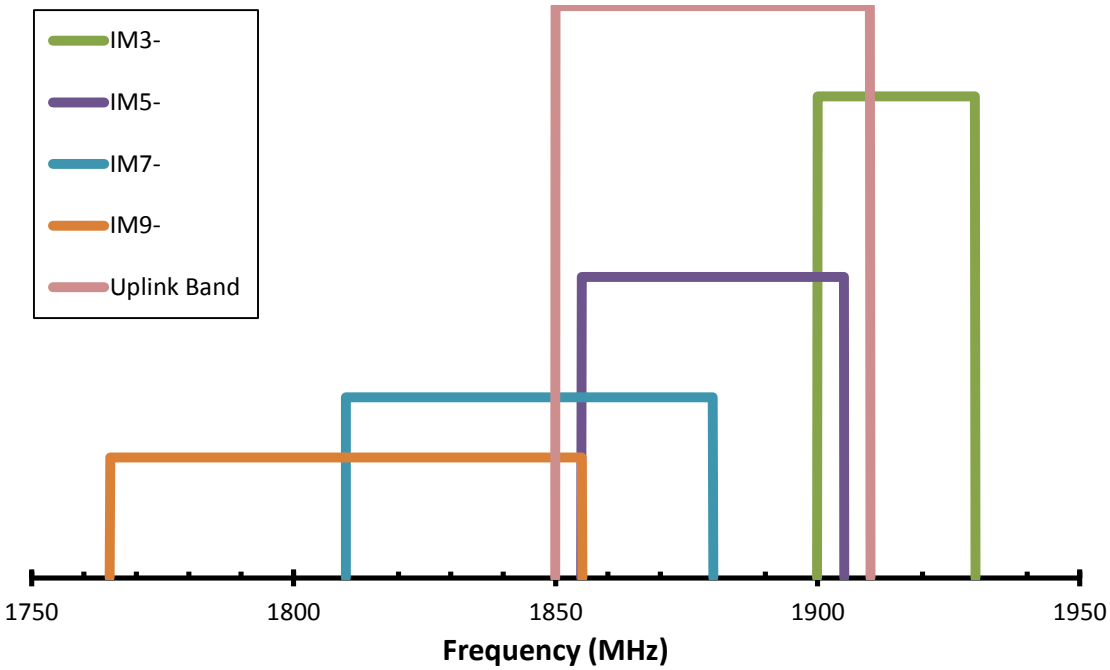

Figure 3.3 *Illustration of the negative IM products falling on E-UTRA band 2 uplink which is the RX band for the base station. CCs, which are not shown in the figure, have 10 MHz bandwidths and the center frequencies are 1950 MHz and 1985 MHz. Negative 3rd, 5th, 7th and 9th order IM products are marked as IM3-, IM5-, IM7- and IM9-.*

The aspect in Figure 3.3 is from the base station side and therefore the RX band frequencies are the same as the uplink frequencies, because the uplink is from the UE to the base station. The same phenomenon also happens in the downlink side, from the base station to the UE, because IM products are generated both sides of the desired signals. As illustrated in Figure 3.3, with narrow the duplex spacing the negative 3rd order and also the negative 5th order IM product can fall on the transceiver's own RX band. In this illustration the CCs center frequencies are 1950 MHz and 1985 MHz, and because the duplex spacing is 80 MHz, the base station RX center frequencies are 1870 MHz and 1905 MHz. The RX frequencies can be calculated by subtracting the duplex spacing from the TX frequencies. To compare duplex spacing width influence, the illustration of IM products at E-UTRA band 1 is shown in Figure 3.4. This example is also from the base station side aspect and again the RX band is the uplink frequencies. Similarly to Figure 3.3, also Figure 3.4 is a simple illustrative example.

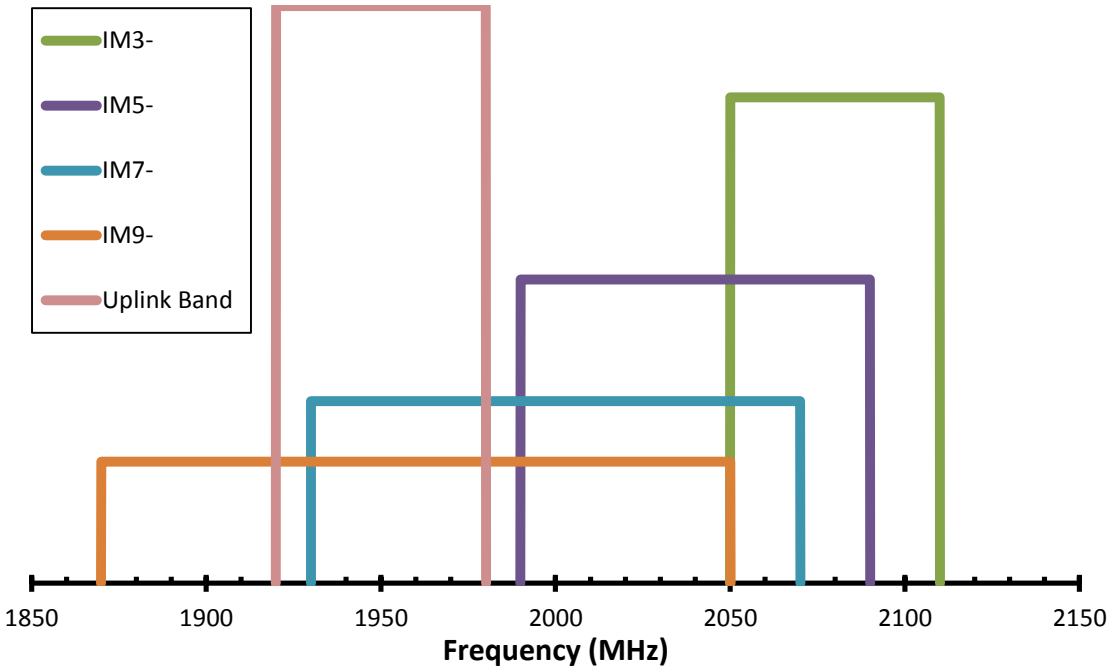

Figure 3.4 *In this illustration for E-UTRA band 1, the CCs bandwidths are 20 MHz and the center frequencies are 2120 MHz and 2160 MHz. The CCs are not shown in the figure, but the negative 3rd, 5th, 7th and 9th order IM products are marked as IM3-, IM5-, IM7- and IM9-. This illustration is from the base station side and it demonstrates that high-power 3rd and 5th order IM products do not fall on RX band even if the CCs are at the edges of the TX band.*

In the case where the duplex spacing is 190 MHz, the 3rd or 5th order IM product do not fall on the RX band area even if the CCs bandwidths are the maximum 20 MHz. Still the 7th and 9th order IM products fall on the RX band, and because of the wide bandwidth they almost cover the whole RX band frequency domain. The RX center frequencies are 1930 MHz and 1970 MHz, because the duplex spacing is 190 MHz and the CCs center frequencies are 2120 MHz and 2160 MHz in this example. In these two illustration examples presented above, the focus is in the base station side, because PIM is more of a base station side problem. However, IM is also a problem in the UE side but usually because of nonlinearities in active circuits like in PA. The aspect was chosen, because this thesis concentrates more on PIM at a base station transceiver.

3.5 Mitigation of Intermodulation Products

To discuss about the mitigation of IM products, it is convenient to introduce a more specific block diagram of an example transceiver, which is shown in Figure 3.5 [5, p. 3]. This example transceiver uses the FDD CA technology and it may contain several nonlinear connectors between different modules of the transceiver, because this example also concentrates on a base station side. In UE there would not be connectors between modules, especially if the UE is a mobile device. Furthermore, the antenna struc-

ture in a base station usually contains metal junctions which can also be the source of PIM.

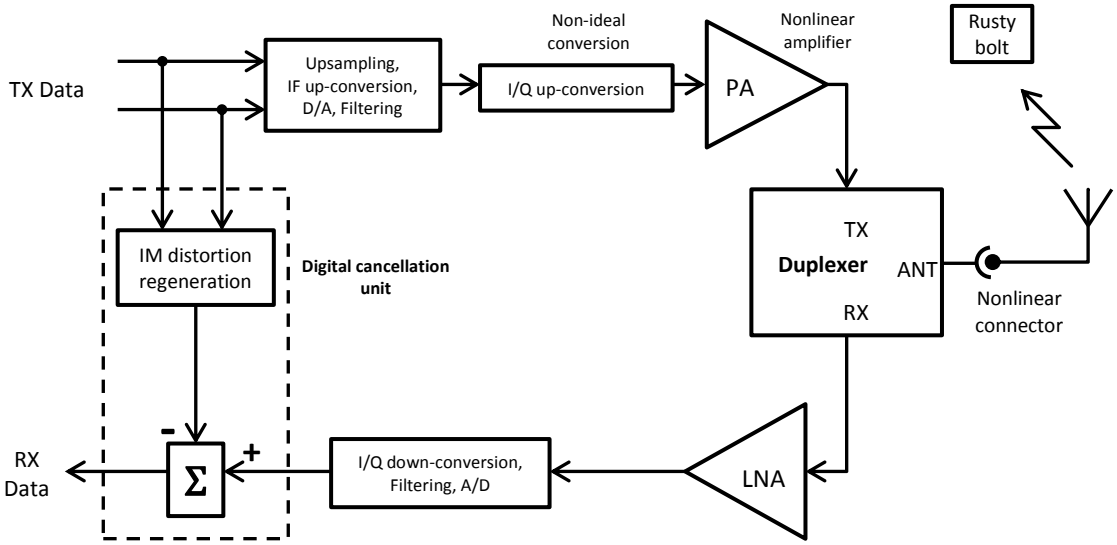

Figure 3.5 *Example block diagram of a CA transceiver containing several IM sources in the system and also outside of the transceiver system in the nearby corroded object.*

As seen from Figure 3.5, there are two TX data signals, because the transceiver is for the LTE CA technology. This example is only a one solution for a CA transceiver implementation and there are several different implementation possibilities. In this solution upsampling, intermediate frequency (IF) conversion and digital to analog (D/A) conversion are done separately for both TX data signals. After this, the signals are combined and in-phase quadrature (I/Q) up-conversion is done with a single I/Q modulator. Finally, the modulated signals are amplified and led into the duplexer's TX port. Other solutions for TX signal modulations could be that the signals are combined at the beginning of the TX chain or at the end of the TX chain before the duplexer [35, p. 24]. If CCs are at different E-UTRA bands, inter-band LTE CA, then it would be reasonable to use implementation where both CCs have completely different TX chains [36, p. 78]. In contiguous intra-band LTE CA, the simplest solution where is only one TX chain may be a good choice, at least it is the least power consuming choice and it has the smallest chip size [36, p. 78]. However, the example shown in Figure 3.5 might be the best choice for non-contiguous intra-band LTE CA, because it is less complicated and expensive than implementation with separated PAs [36, p. 78]. Although in the above solution, the PA has to be as linear as possible because of the wider bandwidth, to avoid high-power IM products.

The RX chain of the transceiver consists of a LNA, an I/Q down-conversion unit and also an analog to digital (A/D) converter. The LNA amplifies the received RX signal which is then demodulated back to digital form. Also a digital cancellation unit and a duplexer are presented in Figure 3.5. The duplexer is explained in more specifics in Subsection 3.5.1 and the digital cancellation unit in Subsection 3.5.2.

3.5.1 Duplexer Isolation

A duplexer is a three-port module, with a TX, RX and antenna port. It has isolation between the TX and RX port, which in ideal case means that TX signals do not go into the RX port and vice versa. This isolation can be implemented with filters and also with a circulator. Filters are band-pass type and with reasonable costs and sizes, the attenuation may be only 50 – 60 dB in mobile transceiver duplexers [5, p. 1]. However, in a base station duplexer, the isolation can be much higher, because the size and the power consumption do not limit the duplexer implementation as much as in mobile transceivers.

Duplexer's band-pass filters can usually filter out easily harmonics and IM products which are far from the desired signals, but odd order IM products may cause problems. Especially in a case where the duplex spacing is narrow, the most high-power 3rd order IM product falling on RX band can cause the transceiver's own RX desensitization. The desensitization can happen because of the finite duplexer isolation. Odd order products can be very close to the band-pass area of the filter and therefore they might not be attenuated enough. Furthermore, the high-power IM product may be transmitted to other receivers if the TX band-pass filter cannot completely filter it out. In addition, the sensitive LNA may become saturated and generate also IM products if the IM products from the TX chain leaks into the RX chain. These problems are even more challenging in mobile UEs, because of the lower isolations in duplexers.

The TX filter can attenuate only IM products which are generated in the TX chain of the transceiver. Furthermore, TX chain contains I/Q modulator which may have imbalance and it may generate unwanted signals from the original signals [5, p. 3]. These unwanted signals are mirror images of the desired signals. The biggest IM source in TX chain is usually a PA which behaves nonlinearly [3, p. 56]. The PA is usually designed to be used close to the saturation to achieve better power efficiency, which increases the IM products power levels. These IM products due to the PA can have high powers, which require high attenuation from the TX filter. Other possible sources of IM are PIM sources, like connectors and damaged cables in the TX chain. At a base station, different modules of the TX chain might be connected to each other with connectors and possibly with considerably long cables which may be damaged and therefore cause PIM. However, these PIM sources have relatively small powers when compared with the IM products due to PA. Also the PIM generated in TX chain can be attenuated with the TX filter, but more problematic sources of PIM are connectors after the duplexer. Because of those connectors, PIM can be generated after the TX filter. If those IM products are at the RX frequency band, then they can leak directly to the RX chain LNA, because the RX filter does not attenuate them. Furthermore, the PIM can be generated in the metal junctions of the antenna structure or even outside of the transceiver system, and those sources of PIM are also after the TX filter.

3.5.2 Digital Cancellation

The digital cancellation unit is shown in Figure 3.5 and the basic idea in digital cancellation is to predict IM products and subtract them from the RX chain by regenerating replicas of these products [3, p. 55]. Because the cancellation is done after the duplexer in the RX chain, also the PIM products which are generated after the TX filter can be cancelled. The main problem in digital cancellation is that IM products amplitudes, phases and delays depend on the used PA, duplexer and other components. Furthermore, these IM products amplitudes and phases are not constants and vary in time. The digital canceller has to model different parts of the transceiver to regenerate IM products. To achieve this, the transmitted data and its frequency are known but the rest of the coefficients in the regeneration have to be estimated [5, pp. 4-6]. There are different modelling techniques and needed coefficients in regeneration depend on the implemented cancellation unit. In the estimation, it is needed to know how the sent TX signal is seen in the RX chain. This can be done by taking and processing samples from the received signal and these samples can be used as a feedback for the estimation [5, p. 7]. Finally, the regenerated IM signal inverse can be added to the RX signal to reduce the actual IM products in the RX band.

The modeling of interference at a certain IM product frequency band contains also higher order IM products estimation [3, p. 64]. Higher order IM products estimation improves digital cancellation, because a certain IM band contains also higher odd order IM products [3, p. 61;64]. Therefore, for example, digital cancellation for 3^{rd} order IM band has to estimate also 5^{th}, 7^{th} and possibly even higher odd order products [3, p. 61;64]. In theory, the more of odd order IM products are estimated, the better interference reduction can be achieved. However, the higher the IM product order is the lower is the power of it and due to that the influence of product decreases as the order number increases. In the measurements of this thesis, the used model in digital cancellation is parallel Hammerstein model which is introduced in more specifics in [5].

The needed parameter estimation for the digital cancellation can be done when the transceiver is not in use or when it is not receiving signals [5, p. 7]. This type of estimation is called offline estimation and the estimated coefficients can be used when the transceiver is in use [5, p. 7]. However, the IM products may vary in time and the estimation has to be done frequently while transmitting to achieve better interference cancellation. It is also possible that the power of the IM interference increases and the transceiver has to be in use while the estimation is done. In this kind of online estimation, the actual RX signal from the other transmitter has to be considered as noise [5, p. 10]. The desired RX signal does not depend on the transmitted signals and therefore it is similar to the independent noise in the aspect of estimation process [5, p. 10]. Nevertheless, if the desired RX signal is strong enough, it will make the estimation more difficult. In this kind of situation the estimation can be improved by increasing the RX signal sample data rate [5, p. 10]. Although, if the RX signal is very strong, the IM prod-

ucts might not interfere the data transmission but it is also possible that both, desired RX signal and IM product signals have high powers.

In conclusion, the digital cancellation can be used to reduce IM products which are at the transceiver's own RX band. The IM products may be generated by different components in the transceiver. The IM products may end up in to the RX chain because they have high power which cannot be completely attenuated with the duplexer's TX filter or they are generated after the TX filter in possible sources of PIM. Benefits in digital cancellation are that it can be used to reduce also the IM products which are generated after the TX filter, and the duplexer filters do not have to have as much attenuation. Filters with high stop-band attenuation have higher insertion loss and also the implementation is more complex which leads to a lower power efficiency and higher duplexer cost.

4. GENERATING PASSIVE INTERMODULATION AND MEASUREMENT SETUP

In this thesis, the scope is to generate PIM after TX filter of the duplexer and then demonstrate that PIM can be reduced with digital cancellation. To achieve this, a base station E-UTRA band 1 PA, duplexer and LNA are used. The problem in these measurements is that PIM is occasional phenomenon and it requires high powers to become significant [6] [7]. PIM cannot be generated with a broken cable or a corroded conductor in these measurements, because it would not be reproducible test setup and measurement results might vary in time. Furthermore, the duplex spacing in E-UTRA band 1 is 190 MHz which is considerably wide. Therefore, the most high-power 3^{rd} order PIM products are not at the RX frequency band and lower than 7^{th} order products do not fall on RX band as seen in Section 3.4 examples. Therefore, the PIM source in the measurements must be very nonlinear to generate 7^{th} and higher order products which have significant power levels. If the PIM source is not generating high-power PIM products, the TX power has to be increased and the duplexer TX filter may not be able to completely attenuate the IM products from the TX chain of the transceiver system. In this kind of situation, it is difficult to know if the digital cancellation decreases only IM products which are generated in the TX chain PA.

To achieve a reproducible test setup, a nonlinear circuit is added between the duplexer and a 50 Ω termination. In these measurements, an actual antenna is not used, because it can also generate PIM products. In addition, to avoid interfering actual mobile transmissions, it is not desired to transmit the test signals over the air. Therefore, the 50 Ω termination is used instead of an antenna. The nonlinear circuit is implemented with a diode and simulations of the circuit and component selections are introduced in the next section. The circuit implementation and layout are introduced in the second section. Finally in the third section, the whole measurement setup is introduced and explained.

4.1 Modelling Passive Intermodulation Source with a Diode

Because E-UTRA band 1 has a wide duplex spacing resulting that lower than 7^{th} order IM products will not fall on the RX band, a highly nonlinear IM source has to be used to generate high-power IM products which could interfere receiver. In this thesis the measurements are done by emulating a nonlinear connection at the antenna port of the duplexer, because nonlinear metal junctions are the most common source of PIM [6] [7]. A thin oxide layer between two metals in the junction can have a diode like behavior [6] [7] and therefore in this thesis, a diode is used in modelling of nonlinear connec-

tion. Also by using the diode circuit, the test setup becomes easily reproducible. A Schottky diode is chosen for this, because the frequency of the E-UTRA band 1 is around 2.1 GHz, which requires fast switching speed from the diode. The Schottky diode is based on semiconductor-metal junction, which decreases the junction capacitance and enables faster switching speed than a normal p-n junction diode [4, p. 509]. The equivalent circuit of a Schottky diode is shown in Figure 4.1 where V_d is the voltage over the diode [4, p. 511].

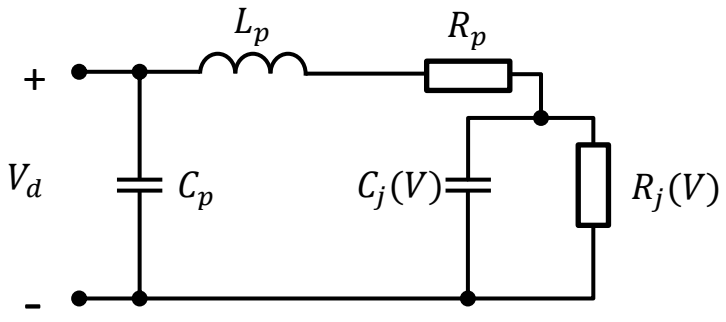

Figure 4.1 *The equivalent model of a Schottky diode consists of parasitic capacitance, inductance and resistance, and also of nonlinear capacitance and resistance which depend on the voltage.*

The parasitic capacitance C_p, inductance L_p and resistance R_p are caused by the structure of the diode and also from the junction between the component and the circuit board [4, p. 511]. The nonlinear resistance $R_j(V)$ and capacitance $C_j(V)$ are modelling the semiconductor-metal junction in the diode [4, p. 511]. The junction capacitance is smaller when the reverse voltage is higher and the resistance varies according to the voltage [37]. As seen from Figure 4.1, the Schottky diode contains also capacitance and inductance which causes phase shift between the voltage and the current of the diode.

To emulate a weak connection between a duplexer and an antenna, the diode is designed to be connected parallel with antenna. The circuit diagram of the diode circuit for IM source is shown in Figure 4.2. The circuit contains SMA connectors in the input and the output port and a transmission line with 50 Ω characteristic impedance between those ports. The BAT54S component contains two Schottky diodes in series in SOT-23 case [37]. The Diodes are connected to the transmission line with series resistance R which limits the current through the diode component. The other diode starts conducting when the voltage is positive and the other when the voltage is negative which makes the circuit behavior similar at positive and negative voltages. As the voltage rise enough at the transmission line, one of the diodes starts conducting. Therefore, part of the power is not delivered to the output port and the higher the input power is the higher is the insertion loss of the circuit. Furthermore, when the impedance of the diode varies, also the

whole load impedance varies. Therefore, the power that is reflected from the input port can increase or decrease.

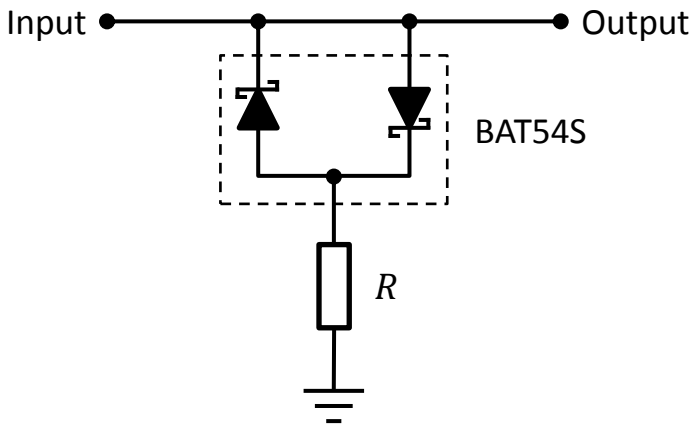

Figure 4.2 *The transmission line between the input and output port is grounded through the BAT54S Schottky diode component and resistor.*

The resistance value of the resistor must be designed so that the current is lower than the maximum current limit of the diode component. Although, with a too big resistance value the circuit might not generate high-power IM products, because the voltage has to be higher before the diode starts conducting. However, as seen in Figure 4.1, a Schottky diode contains also parallel capacitance which means that the diode might conduct high frequency signals through the parallel capacitance. The maximum repetitive peak forward current for the BAT54S component is 200 mA and 30 V is the maximum repetitive peak reverse voltage for the component [37]. The circuit is simulated with LTspice IV program to find out what are the currents and voltages in the circuit with different input powers. The simulations were done with resistor values of 50 Ω and 100 Ω and the simulation results are shown in Table 4.1, which shows that the maximum input power to the circuit is +33.8 dBm when a 50 Ω resistor is used and +38.1 dBm when a 100 Ω resistor is used. With these input power values, the peak current of the diode is at the maximum value. Therefore, these input power values should not be exceeded. However, these values are only simulations and the real current values may vary due to the power reflections and tolerances of the resistor and the diode component. Furthermore, these simulations do not take into account the resistor parasitic capacitance or inductance. Also the junctions between the components and the circuit board have parasitic elements which are not taken into account in the simulations. The dissipated power in the resistor is also shown in Table 4.1, which shows that the 50 Ω resistor power rating has to be at least 1 W and the power rating for the 100 Ω resistor has to be at least 2 W.

Table 4.1 *The currents and voltages in the circuit according to the simulations with LTspice IV program. The maximum peak current is 200 mA for the BAT54S component, which means that the maximum powers for the diode circuits are +33.8 dBm for the 50 Ω resistor diode circuit and +38.1 dBm for the 100 Ω resistor diode circuit.*

Resistor value (Ω)	Diode peak current (mA)	Diode peak voltage (mV)	Resistor power (W)	Output peak voltage (V)	Input power (dBm)
50	200	645	1.0	10.5	33.8
100	122	427	0.74	12.4	33.8
100	200	645	2.0	20.5	38.1

The circuit in the simulations was the same as the one shown in Figure 4.2 and in the input port was a sine voltage source with a 50 Ω series resistance and 2.1 GHz frequency. The output port was terminated with a 50 Ω resistor. The voltage source amplitude had to be solved from the input powers for the simulations. Equation (4.1) shows which is the maximum power to the load if the load is perfectly matched to the generator [4, p. 79]. In this case the load resistance was assumed to be 50 Ω which is the same with the generator series resistance.

$$P_L = \frac{|A_g|^2}{8R_g} \tag{4.1}$$

The power delivered to the load is P_L in watt units, amplitude of the generator is A_g and R_g is the 50 Ω series resistance of the generator. With a perfectly matched load, only half of the power is delivered to the load and the other half is dissipated in the series resistance of the generator. Therefore, the output voltage amplitude of the generator is only a half of the generator amplitude shown in Equation (4.1) [4, p. 79].

$$A_g = \sqrt{8P_L R_g} \tag{4.2}$$

Equation (4.2) is solved from Equation (4.1). The equation is used to calculate the amplitude values for the voltage source in the simulations. In Table 4.2 the maximum input powers from Table 4.1 in units of dBm and W are shown. Also the generator amplitude, which is calculated with Equation (4.2), is shown in Table 4.2.

Table 4.2 *Relation between the input power and generator amplitude. Generator amplitude is not the same with generator output voltage, because the generator has 50 Ω series resistance.*

Input power (dBm)	Input power (W)	Generator amplitude (V)
+33.8	2.4	31
+38.1	6.5	51

These voltage values related to the input powers do not take into account the load impedance change which is caused by the diode component and resistor. These calculated values expect that the load impedance is 50 Ω, which is the same as the generator impedance. However, by using these values in the simulations it gives a good estimation about the electrical parameters for choosing the components to the circuit. Furthermore, when the circuit impedance is not perfectly matched to 50 Ω, a lower power is delivered to the circuit than what was simulated. Therefore, the components which are chosen based on these simulations can be used at least with these powers shown in Table 4.2.

4.2 Implementation of the Diode Circuit

According to the simulations done with LTspice IV program, the resistors have been chosen to be Bourns CHF2010CNP500LX and CHF2010CNP101RX which both are rated for 10 W maximum powers [38]. The first is a 50 Ω and the second is a 100 Ω radio frequency (RF) resistor and both are in 2010 cases [38]. For circuit implementation, it is needed to calculate the transmission line width for a microstrip with a 50 Ω characteristic impedance. The width of the microstrip transmission line is calculated with Advanced Design System program's LineCalc tool. With the parameters shown in Table 4.3 the calculated width is approximately 3.06 mm, for the 50 Ω characteristic impedance transmission line.

Table 4.3 *The parameters which are used in Advanced Design System LineCalc tool for calculating the width of the microstrip line. Frequency is 2.1 GHz which is between the uplink and downlink frequency bands in E-UTRA band 1.*

Characteristic impedance (Ω)	50
Frequency (GHz)	2.1
Relative permittivity	4.3
Substrate thickness (mm)	1.6
Substrate loss tangent	0.02
Conductor conductivity (S/m)	5.8e7
Frequency of defined loss tangent (GHz)	9.4

The calculated width for the 50 Ω characteristic impedance is approximately the same 3.06 mm at the uplink and downlink frequencies of E-UTRA band 1. The circuit board which is used is a FR4 double sided circuit board. The fabricated diode circuit is shown in Figure 4.3.

Figure 4.3 *The fabricated circuit with the BAT54S diode component and 50 Ω RF resistor which is grounded through the circuit board on the left side of the board. The input and output port have SMA connectors and because the circuit is physically symmetrical, the circuit is also reciprocal and it does not matter which port is the input or the output port.*

As seen from the layout, the transmission line with 50 Ω characteristic impedance is between the input and output port and the diode component is connected directly on the middle of the transmission line. There is also a 50 Ω transmission line between the diode component and the RF resistor. The length of the transmission line between the ports is 23 mm and 5 mm between the diode and the resistor. The other end of the resistor is connected to a conductor area whose length and width are 8 mm. The conductor area is designed to be large enough for grounding through the circuit board to the ground layer which is the bottom layer of the circuit board. Because the circuit is symmetrical, it is not significant which one of the SMA connectors is the input or the output port.

Diode circuit boards were made for both resistor values, for the 50 Ω and 100 Ω RF resistors. The circuit layout was the same for both circuit boards, because the diode component is the same and the case of the resistor is the same with both resistors.

4.3 Measurement Setup

As introduced in Section 2.6, PIM can be measured with the reverse and forward measurement. In this thesis, the measurements are done with the reverse PIM measurement, because it is more suitable for measuring PIM which is generated at the antenna port of the duplexer. Furthermore, the forward measurement is more suitable for measuring component's PIM generation while in this thesis the interest is on the PIM power levels which appear in the RX port of the duplexer. Furthermore, only the reflected IM products can desensitize the transceiver's receiver or can be digitally cancelled. The forward measurement would also require an isolator or a coupler after the PIM source and the

isolator or the coupler could also generate IM products. Therefore, the reverse measurement is used in this thesis.

Figure 4.4 shows the measurement setup which was used in the measurements of this thesis work. The measurement setup contains a PA, duplexer, LNA, PIM source circuit and National Instruments vector signal transceiver (VST). The VST is controlled by MATLAB program and the antenna is replaced with a 50 Ω termination. An antenna is not used, because test signals generated by VST could create interference to commercial mobile networks. Furthermore, an antenna could also generate PIM products and therefore measurement results could vary, if the measurement is repeated with a different antenna. The duplexer, PA and LNA are integrated together and designed for E-UTRA band 1 base station use. E-UTRA band 1 has considerably wide 190 MHz duplex spacing and therefore the IM products, whose frequencies are at RX band, are 7^{th} or higher order IM products, which was shown in example in Section 3.4. Because the power level of the IM product decreases when the order number increases, the measurements and digital cancellation are focusing on the 7^{th} order IM product which has the highest power at the RX band.

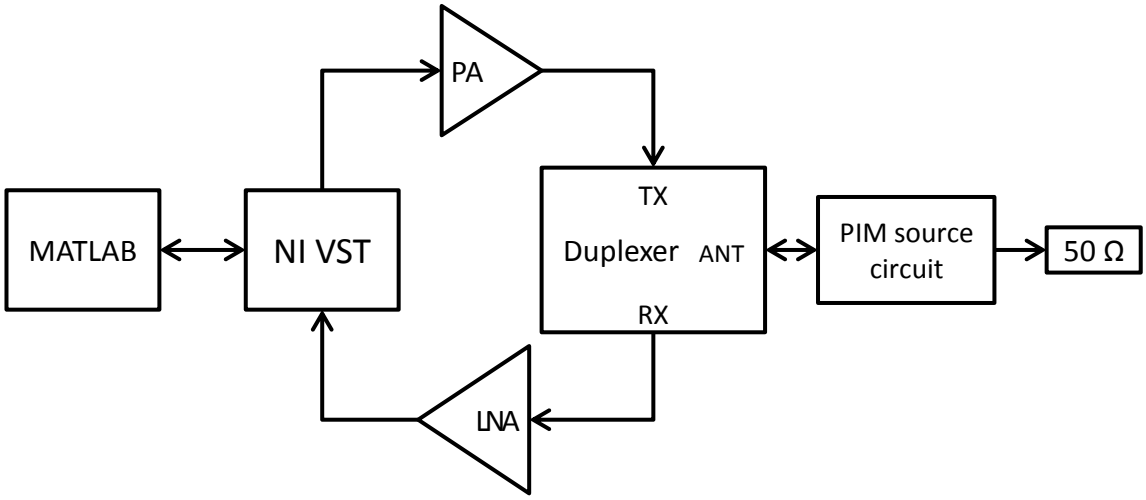

Figure 4.4 *The block diagram of the measurement setup. A 50 Ω termination is used instead of an antenna and the PIM source is located between the duplexer and the termination.*

As seen from Figure 4.4, the VST is controlled with MATLAB program. The VST generates LTE CA signals which are fed into the PA and then to the duplexer. Because the duplexer is designed for a base station use, the isolation between TX and RX port is considerably high. Therefore, the IM products due to the PA are filtered out and only the IM products due to the PIM source circuit are seen at the RX port of the duplexer. However, it is still possible that the IM products due to the TX chain PA leak into the RX port if the input power is high enough. Because of that, the system noise floor has to be measured without the PIM source circuit, to see if IM products appear at the RX port without the circuit. The LNA cannot be bypassed because the LNA, PA and duplexer

are integrated together. Therefore, the gain of the LNA, which is 31 dB, has to be subtracted from the measurement results to get the power levels at the RX port of the duplexer. After the LNA, the signals are fed back to the VST and the results are taken to MATLAB program. The digital IM cancellation is done with MATLAB program and also the measurement results can be visualized with it.

It is also possible to add an external PA between the VST and the PA shown in Figure 4.4, to achieve higher TX power to the PIM source. However, the diode circuit is very nonlinear and generates powerful IM products and therefore an external PA is not required. But if the PIM products are generated with a loosely connected SMA connector, then the TX power at the antenna port has to be much higher and the external PA is required. In this thesis, also measurements with a loosely connected connector are done to show that even 7^{th} and 9^{th} order PIM products may have high power levels and to compare these power levels to the IM power levels which are generated with the diode circuit. However, generating high-power PIM products with a loose connector is difficult because with a too tight connection there are not much gaps between the metal surfaces and the tunneling effect will not affect as much to the connection resistance. Furthermore as said in Subsection 2.3.1, the probability for the tunnel effect decreases significantly if the insulating layer or the air gaps are wider than 10 nm. Therefore, a too loosely connected connector does not generate powerful PIM products, because the gaps in the junction are too wide and the probability for electron tunneling is low. In conclusion, to generate 7^{th} and 9^{th} order PIM products with a SMA connector, the connector has to be optimally loosened and high input power has to be used.

5. MEASUREMENT RESULTS AND ANALYSIS

In this chapter, the measurement results which are done with the test setup introduced in Section 4.3 are introduced. The measurements were done with an E-UTRA band 1 base station duplexer, PA and LNA, and for both diode circuits. In these measurements, the TX power at the antenna port of the duplexer was varied from +11 dBm to +32 dBm. For a loose connector spectrum measurement, there was an external PA included to the measurement setup input and the TX power at the antenna port was increased to +39 dBm.

First, in this chapter, the measured 7^{th} and 9^{th} order IM product powers with two diode circuits are presented. Also the spectrum of the LNA output with the 50 Ω resistor diode circuit is presented. After that, the spectrum with a proper and a loose SMA connector in the antenna port of the duplexer is shown for the comparison to the diode circuit generated IM products. Finally in this chapter, the results of the digital 7^{th} order IM cancellation for both diode circuits are given.

5.1 Power of Intermodulation Products

In these measurements, a base station duplexer, PA and LNA for E-UTRA band 1 was used. The duplexer has 190 MHz duplex spacing and therefore only 7^{th} and 9^{th} order IM products are measured in the following measurements. First was tested that IM products power levels are close to the same when one CC frequency was changed. Because there were not significant difference in the IM products power levels with different CC frequencies, following measurements were done only with the same frequencies. The downlink of the E-UTRA band 1 is 2110 – 2170 MHz [23, p. 28] and therefore CCs center frequencies were chosen to be 2114 MHz and 2162 MHz. The bandwidths are 1.4 MHz for both CCs and with these frequencies the negative 7^{th} order IM product center frequency is 1970 MHz, and 1922 MHz is the center frequency of the negative 9^{th} order IM product. Because the uplink of the E-UTRA band 1 is 1920 – 1980 MHz [23, p. 28], both 7^{th} and 9^{th} order IM products are at the base station duplexer's RX frequency band. OFDMA with QPSK modulation was used for TX data, because the measurements are concentrated to the base station side and OFDMA is in use at downlink data transmission in the LTE CA technology.

In Figure 5.1 the powers of IM products at the duplexer's RX port are shown related to the TX power at the antenna port of the duplexer. The TX power is varied from +11 dBm to +32 dBm and the measurement bandwidth is 10 MHz. The powers in Figure 5.1 are measured with the diode circuit which has the 50 Ω resistor, but the black

curve in the figure is measured by replacing the diode circuit with a SMA adapter. The results from the measurement without the diode circuit show that the isolation between the duplexer's TX and RX port is high enough to completely filter out the IM products generated in the TX chain. Therefore, the power at the RX port is constant with all TX powers when the measurement is done without the diode circuit. The powers are measured from the LNA output port as shown in Figure 4.4, but results in Figure 5.1 are referred to the input port powers of the LNA which are calculated by subtracting 31 dB, which is the gain of the LNA, from the measurement results.

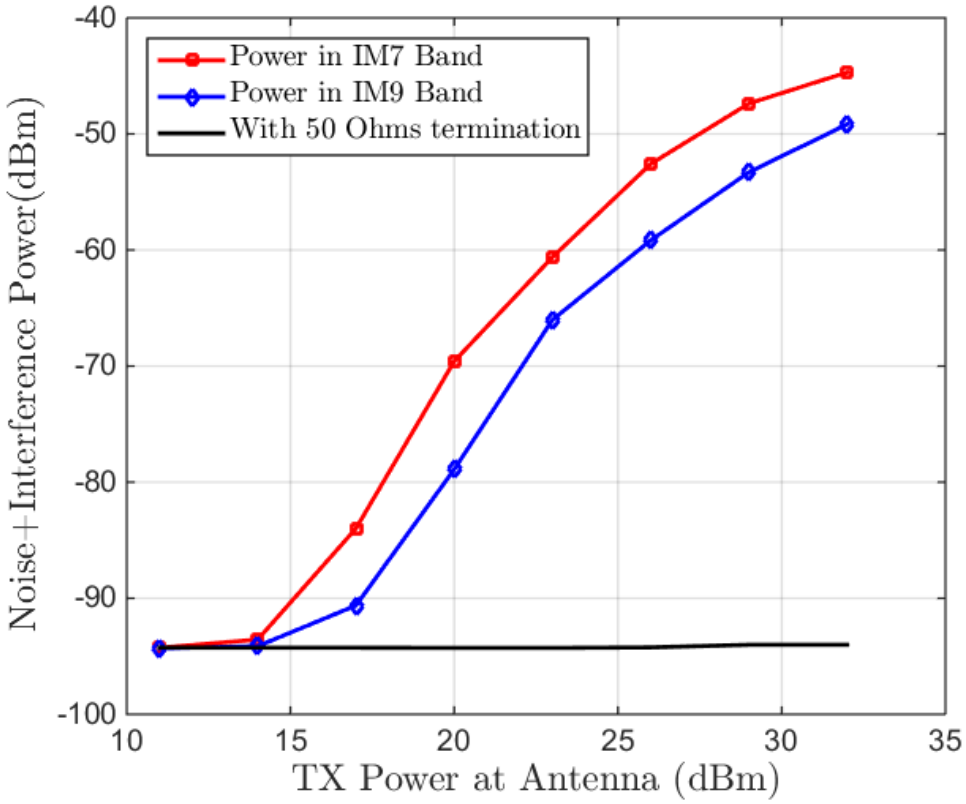

Figure 5.1 *The negative 7th and 9th order IM product power levels of the diode circuit with the 50 Ω series resistor. These powers are referred to the RX port of the duplexer and with the 50 Ω termination the diode circuit was replaced with a SMA female-female adapter.*

As seen from Figure 5.1, the IM products powers increase quickly when the TX power is increased. As introduced in Section 2.2, the power of IM product should increase by the order number when the desired output power increases 1 dB. However, in this case the powers do not increase with the slope of 7 or 9. The explanation for this might be that the parasitic properties of the diode change when the power is increased. As seen in Figure 4.1, the diode contains parasitic inductance, capacitance and also junction capacitance which depend on the voltage over the diode. The junction capacitance of the diode decreases when the reverse voltage increases, and when the voltage is over 8 V the junction capacitance becomes more stable and does not decrease much [37]. Anoth-

er reason might be that the resistance of the diode varies differently at different voltage levels [37]. Furthermore, when the diode impedance changes also the total load impedance changes and the reflected power may increase. However, in this thesis the main interest is in the digital cancellation of the IM products and therefore the reason for the varying IM product power increase was not studied in more specifics.

In Figure 5.2 the results of the same measurement with the diode circuit containing the 100 Ω resistor are given. As seen from Figure 5.1 and Figure 5.2, the powers of IM products are approximately less than 3 dB higher with the diode circuit containing the 100 Ω resistor. From the same figures can be seen that the IM products powers changes similarly with both resistors, which is expected when the diode component is the same model in both circuits and also the layouts in both circuits are the same.

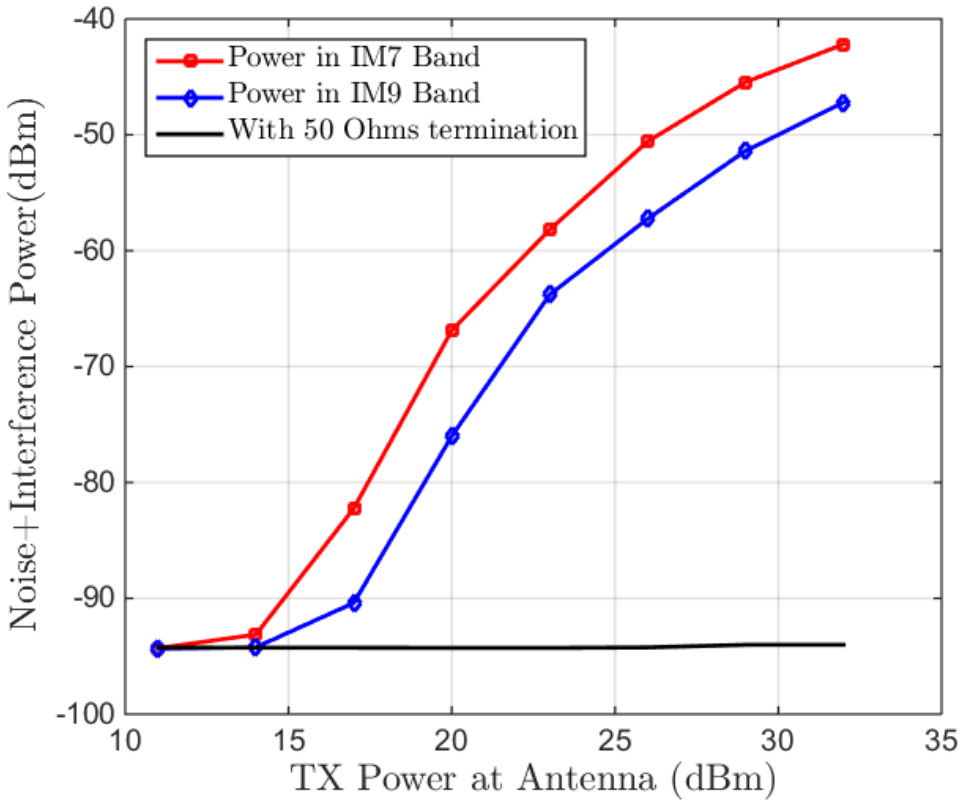

Figure 5.2 *IM products powers with the 100 Ω diode circuit. Similarly to the 50 Ω diode circuit, the 50 Ω termination curve was measured by replacing the diode circuit with the SMA adapter to get the residual IM power level of the test system.*

Figure 5.1 and Figure 5.2 show that both diode circuits are highly nonlinear and therefore already with +20 dBm TX power at the antenna port, both 7^{th} and 9^{th} order IM products have high powers.

To give better understanding of the IM products due to the diode circuit containing the 50 Ω resistor, the spectrum of the LNA output was measured from 1.9 GHz to 2.3 GHz

with +20 dBm TX power at the duplexer's antenna port. The spectrum is shown in Figure 5.3 where the CCs are marked as CC1 and CC2. The negative 7th and 9th order IM products are marked as IM7- and IM9- in Figure 5.3. With the +20 dBm TX power at the antenna port, the negative 7th order IM product can have even more power than CCs which are attenuated by the RX filter. The attenuation of the RX filter is approximately 91 dB, because the gain of the LNA is 31 dB and the powers of CCs at the antenna port are +20 dBm and -40 dBm at the LNA output port. Other IM products are not seen with this TX power level, because they are attenuated by the filters of the duplexer. It is also seen from Figure 5.3 that the bandwidth of the IM products increases slightly when compared to the bandwidths of the CCs. However, the bandwidth increase is not seen very well because the CCs bandwidths are only 1.4 MHz and the spectrum is 400 MHz wide. It is also notable that CCs and IM products do not have as simple rectangular forms as in simplified illustrations in Sections 2.5 and 3.4 examples.

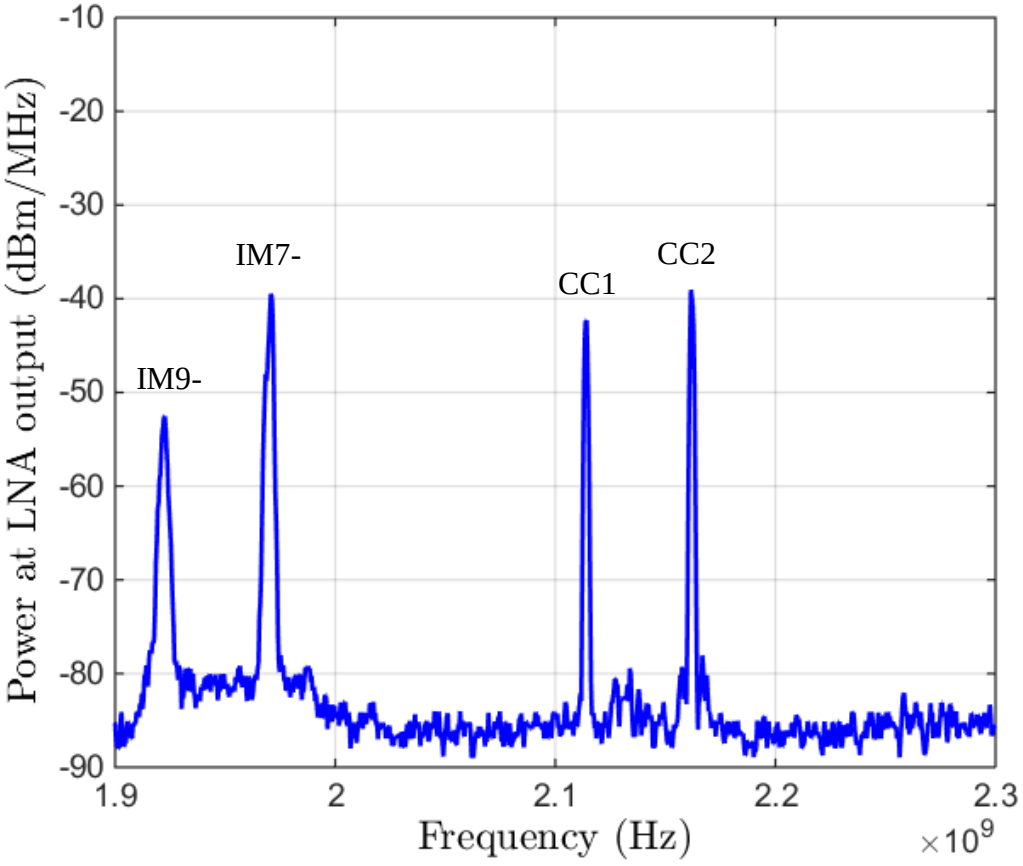

Figure 5.3 *The spectrum at the output port of the LNA with +20 dBm TX power at the antenna port and with the diode circuit containing the 50 Ω resistor. CCs are marked as CC1 and CC2, and the negative 7th and 9th order IM products with IM7- and IM9-.*

For a comparison, PIM was generated and measured with a loose SMA connector at the antenna port. The measurement is not as reproducible as the measurement with the diode circuit, but it shows that even 7th and 9th order PIM products can cause interference to the transceiver's own receiver. Because generating PIM with a loose connector re-

quired higher TX power than with the diode circuit, an external PA was added in the input of the test setup. Therefore, more of the IM products are seen in the spectrum and the measurement with a proper connection shows that part of those IM products are generated in the TX chain PAs. The spectrum is shown in Figure 5.4 where the TX power at the antenna port was +39 dBm, and CCs and IM products are marked like in Figure 5.3. It is seen that the PIM require much higher TX power to appear and still PIM products powers are lower than with the diode circuit. However, the PIM product orders are considerably high and it is difficult to loosen the connection optimally. Because the probability for electron tunneling decreases when the gap between metal surfaces is wider than 10 nm [6], the connector cannot be loosened too much. Therefore, it might be possible to get even higher powers for PIM products with the TX power that was used, if the connector has been tighten with a different torque.

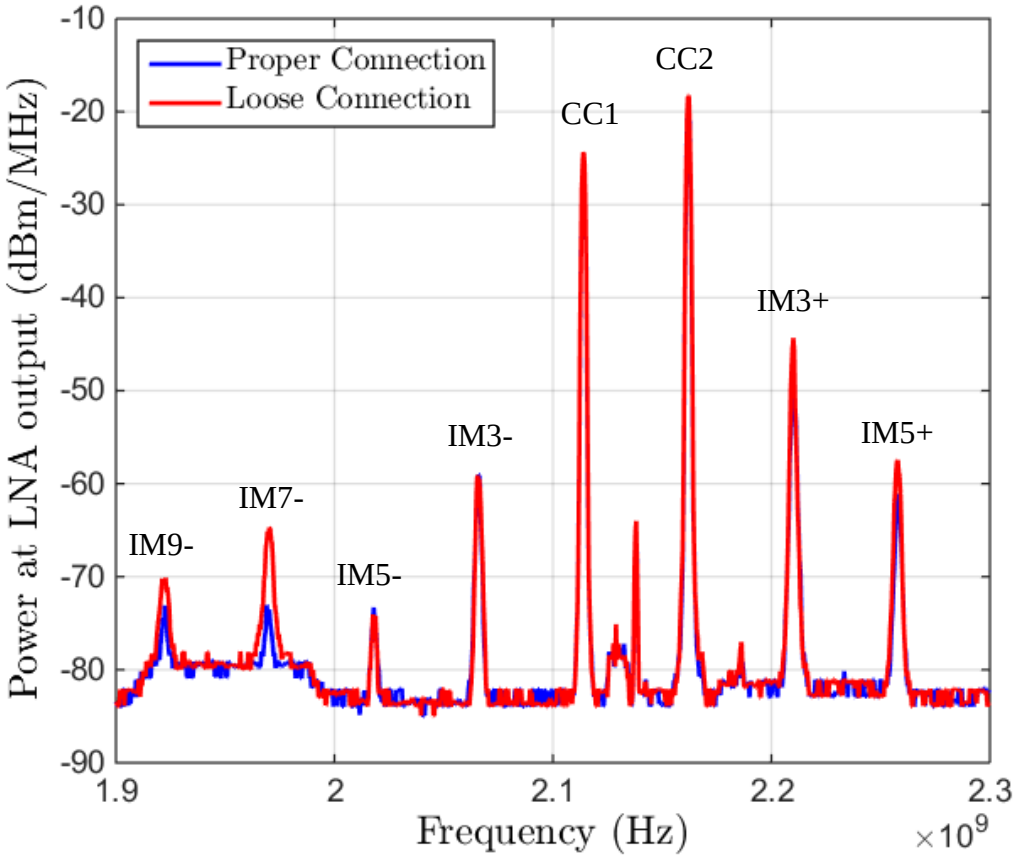

Figure 5.4 *The spectrum from the LNA output with +39 dBm TX power at the antenna port and with a proper and a loose connection in the antenna port cable. Because of the high TX power and another PA in TX chain, also IM products due to PAs are seen in the spectrum. The negative 3rd, 5th, 7th, and 9th order products are marked as IM3-, IM5-, IM7- and IM9-, and the positive 3rd and 5th order products with IM3+ and IM5+.*

By comparing the loose and proper connection spectrums shown in Figure 5.4, it is seen that negative 7th order PIM product has 8.3 dB higher power with the loose connection and 3 dB higher power at the negative 9th order frequency. With other PIM products

seen in Figure 5.4 the difference between the loose and proper connection is not as big as with the 7^{th} and 9^{th} order, because 3^{rd} and 5^{th} order products are attenuated by the RX filter.

In conclusion, the diode circuit is highly nonlinear and generates powerful IM products which can be seen in the spectrum of the duplexer's RX port without seeing IM products due to the PA. PIM can be generated with a loose connector but it requires much higher TX powers and therefore also the IM products due to the TX chain PAs are seen in the spectrum. Also it is difficult to optimally loosen the connector to achieve high-power PIM products and the test setup with a loosened connector is not easily reproducible without knowing the torque of the connection. This also demonstrates that PIM might not be problem with E-UTRA bands which has wide duplex spacing, but instead in the bands where 3^{rd} and 5^{th} order PIM products fall on the RX frequency band.

5.2 Digital Cancellation of Passive Intermodulation Products

Digital cancellation for emulated PIM products is done for both diode circuits with the same TX powers from +11 dBm to +32 dBm at the antenna port. The cancellation is using parallel Hammerstein model which is introduced in [5]. The cancellation is done for the negative 7^{th} order IM product frequency band by estimating 7^{th}, 9^{th}, 11^{th}, 13^{th}, 15^{th} and 17^{th} order IM products.

The digital IM cancellation results for the diode circuit containing the 50 Ω resistor are shown in Figure 5.5. The measurement results are referred to the RX port by reducing the gain of the LNA (31 dB) from the results. As seen from the figure, the emulated PIM interference reduction is the worst with the +32 dBm TX power and the best with the +20 dBm TX power at the antenna port, if the TX powers +11 dBm and +14 dBm are not taken into account. With those two lowest TX powers the IM power is not significant and the reduction is small because the interference is attenuated to the system noise floor level. The lowest reduction is approximately 5.7 dB and the highest is 14.8 dB.

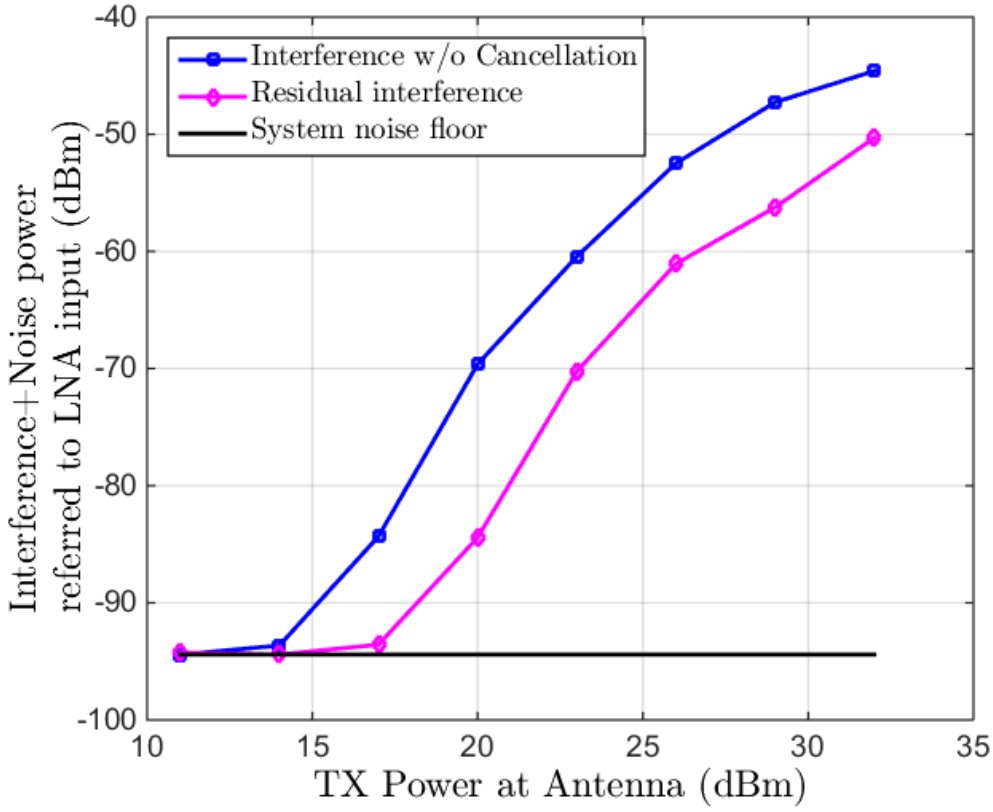

Figure 5.5 *Digital cancellation of the negative 7th order IM product frequency band. PIM is emulated with the 50 Ω resistor diode circuit at the antenna port. With low TX powers the interference can be attenuated close or below the system noise floor.*

In Figure 5.6, the measurement results for the other diode circuit which contains the 100 Ω resistor are given. As seen from the figure, the IM product powers are a little higher, but the results are similar when compared to the measurement with the 50 Ω resistor diode circuit. Again, if two lowest TX powers are not taken into account, the lowest interference reduction is approximately 5 dB and the highest reduction is 9.1 dB which is a little worse mitigation than with the 50 Ω resistor diode circuit but also the interference power is higher.

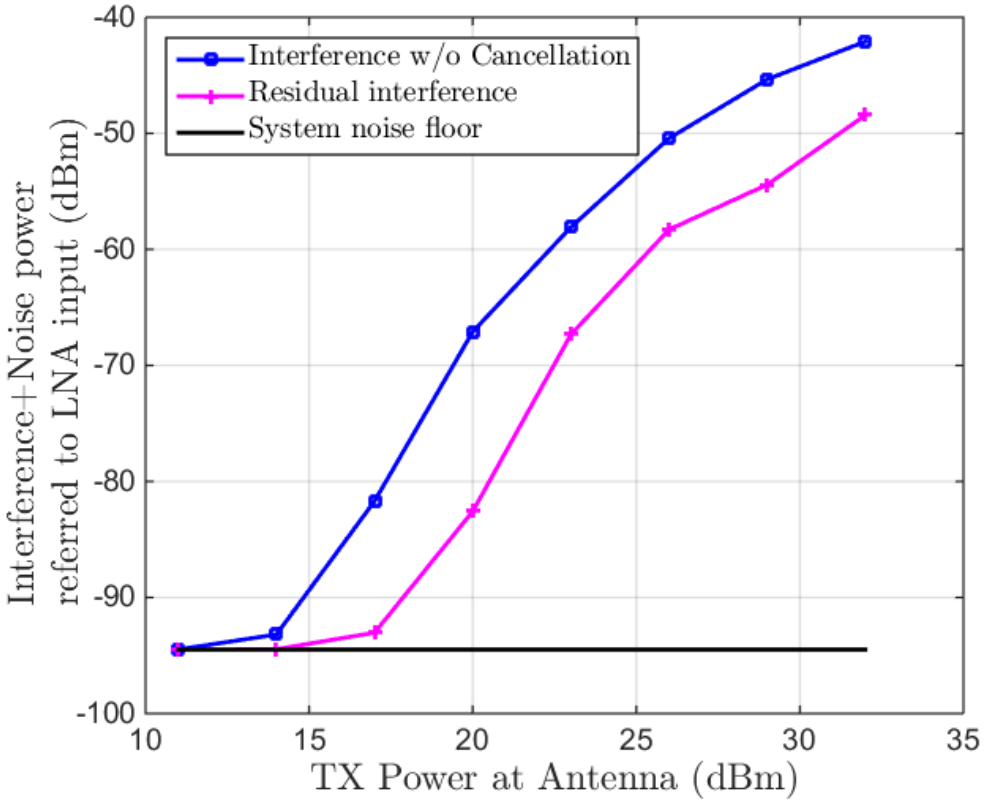

Figure 5.6 *Digital cancellation of the negative 7th order IM product with the 100 Ω resistor diode circuit. Again, with the low TX powers the digital cancellation reduces IM interference close or below the system noise floor.*

The results of the digital IM cancellation with both diode circuits are shown in Table 5.1. The results are shown as interference attenuation for different TX powers with both circuits. As seen from Table 5.1, with the TX powers +11 dBm and +14 dBm at the antenna port the attenuation is small, because the IM product power is very low or it is below the noise floor. Therefore, with these TX powers the digital IM cancellation attenuates the IM down to the system noise floor level or at least close to it. With the higher TX powers the attenuation varies slightly and therefore these measurements should be done again several times to get more accurate average of the effect of digital cancellation.

Table 5.1 *The results of the digital cancellation of the negative 7th order IM product for both diode circuits. The results are presented as interference attenuation in dB units for different TX powers at the antenna port.*

TX Power (dBm)	**+11**	**+14**	**+17**	**+20**	**+23**	**+26**	**+29**	**+32**
50 Ω diode circuit (dB)	0.0	0.7	9.2	14.8	9.8	8.6	9.0	5.7
100 Ω diode circuit (dB)	0.1	1.1	8.2	9.1	5.6	6.7	5.9	5.0

These results demonstrates that it is possible to reduce PIM interference with digital cancellation, but to achieve more attenuation, even higher order PIM products estimation has to be done. However, the emulated PIM powers in these measurements are high for a 7^{th} order PIM product and it might be that PIM due to loose connector does not generate as high powers in 7^{th} or 9^{th} order PIM product bandwidth. Therefore, more measurements have to be done to get better average of the interference attenuation with digital cancellation and also to see how much the most high-power 3^{rd} order PIM products can be attenuated. For this, a duplexer with a narrow duplex spacing is needed. The duplex spacing has to be selected so that the most high-power 3^{rd} order PIM product falls on the RX frequency band.

6. CONCLUSION

The purpose of this thesis work was to demonstrate that the interference due to PIM can be reduced with digital PIM cancellation. The measurements were done with a base station duplexer, PA and LNA because PIM is more of a base station side issue. At the base station, the TX power can be high enough to generate powerful PIM products, and connectors and antennas containing metal junctions are also used in base stations. Existing digital cancellation model and algorithms were used to mitigate emulated PIM products which were generated at the antenna port of the duplexer with a diode circuit. Digital cancellation was tested with different TX powers and with two IM generation circuits. The test setup used the LTE intra-band non-contiguous CA technology, which is vulnerable for IM problems.

To achieve a reproducible test setup, a nonlinear connection in the transmission line was emulated with a diode circuit. The diode circuit was designed to model a nonlinear metal connection, because the most common sources of PIM are loosely connected connectors. Two diode circuits were designed and implemented which both had the same layout and the diode component which contained two Schottky diodes in series. The circuit contained transmission line and part of the input power was delivered through the diode component and a RF resistor to the ground. The difference between the circuits was the resistance value of the resistor, another circuit contained a 50 Ω resistor and the other contained a 100 Ω resistor. In the measurements, LTE CA signals with 1.4 MHz CC bandwidths were generated by VST and fed into a test system containing PA, duplexer and LNA. System was for E-UTRA band 1 which has 190 MHz duplex spacing and therefore the cancellations were done for the negative 7^{th} order IM product which center frequency was at the RX band. Furthermore, lower than 7^{th} order products are not at the RX band and therefore the highest IM product power at the RX band was with the 7^{th} order product. The digital cancellation was done with the MATLAB program which also commanded the VST.

The measurements were done with the TX powers from +11 dBm to +32 dBm at the antenna port for both diode circuits. The same measurement was done also without the diode circuit which showed that the TX filter of the duplexer attenuated completely the IM products from the TX chain PA with these TX powers. The results demonstrated that it is possible to reduce PIM with digital PIM cancellation, but more studies have to be done. With both diode circuits the interference reduction was at least 5 dB, and even 14.8 dB reduction was achieved with the 50 Ω resistor diode circuit when +20 dBm TX power at the antenna port was used. However, the IM products powers were high and more reduction would be needed. In theory, better reduction could be achieved by esti-

mating higher order IM products in digital cancellation, because certain IM product band contains also higher order IM products. Although, the measurements with a loosely connected connector showed that it is difficult to generate very high-power 7^{th} order PIM products. For generating PIM products with a loose SMA connector, an external PA in the input was required, which leaded to the situation where also IM products due to the TX chain PAs were seen at the RX port of the duplexer.

For future research it would be important to do more measurements to achieve more accurate averages of the IM interference attenuation with different TX powers. Furthermore, it is important to study more about the PIM power levels in loose connectors, which are the most common source of the PIM. It is possible that 7^{th} and higher order PIM products are not causing problems and therefore this PIM issue is relevant only in base stations with narrow duplex spacing. Nevertheless, it is important to carry out the measurements, which were done in this thesis, also with a base station duplexer which has a narrow duplex spacing. With narrower duplex spacing, also 3^{rd} and 5^{th} order IM products can be measured. Furthermore, 3^{rd} order PIM products could be generated in a loose connection with lower TX power and without seeing PA's IM products in the RX chain of the transceiver.

In addition for future research, to achieve more reproducible measurements with a loosely connected connector, a wrench with tunable torque could be needed to know what the torque of the connection is. Furthermore, if a reproducible test setup for a loose connection can be achieved, it would be interesting to study how PIM interfere data transmission. This could be studied by including a vector signal generator to the antenna port. Those measurements could be also tested with different modulations like 16-QAM and 64-QAM which are also used in the LTE CA technology and which are more vulnerable for interference.

REFERENCES

[1] ITU-R, "Requirements related to technical performance for IMT-Advanced radio interface(s)," 2008.

[2] J. Wannstrom, "LTE-Advanced," 3GPP, June 2013. [Online]. Available: http://www.3gpp.org/technologies/keywords-acronyms/97-lte-advanced. [Accessed 16 November 2015].

[3] A. Kiayani, Modeling and Digital Mitigation of Transmitter Imperfections in Radio Communication Systems, Tampere: Tampere University of Technology, 2015.

[4] D. M. Pozar, Microwave Engineering, 3rd ed., United States of America: John Wiley & Sons, 2005, 700 p.

[5] A. Kiayani, M. Abdelaziz, L. Anttila, V. Lehtinen and M. Valkama, "Digital Mitigation of Transmitter-Induced Receiver Desensitization in Carrier Aggregation FDD Transceivers," *IEEE Transactions on Microwave Theory and Techniques*, vol. 63, no. 11, pp. 3608-3623, September 2015.

[6] Anritsu, "Understanding PIM," [Online]. Available: http://www.anritsu.com/en-US/test-measurement/solutions/en-us/understanding-pim. [Accessed 17 November 2015].

[7] P. L. Lui, "Passive intermodulation interference in communication systems," *Electronics & Communication Engineering Journal*, vol. 2, no. 3, pp. 109-118, June 1990.

[8] A. Jeffrey, Handbook of Mathematical Formulas and Integrals, 2nd ed., United States of America, San Diego: Academic Press, 2003, 460 p.

[9] T. Lähteensuo, "Linearity Requirements in LTE-Advanced Mobile Transmitter," M.Sc. thesis, Tampere University of Technology, Finland, May 2013. [Online]. Available: http://URN.fi/URN:NBN:fi:tty-201305221148. [Accessed 18 November 2015].

[10] J. Walker, Handbook of RF and Microwave Power Amplifiers, 1 ed., United Kingdom, Cambridge: Cambridge University Press, 2012, 643 p.

[11] A. J. Christianson, J. J. Henrie and W. J. Chappell, "Higher Order Intermodulation Product Measurement of Passive Components," *IEEE*

Transactions on Microwave Theory and Techniques, vol. 56, no. 7, pp. 1729-1736, June 2008.

[12] V. Golikov, S. Hienonen and P. Vainikainen, "Passive intermodulation distortion measurements in mobile communication antennas," *IEEE VTS 54th Vehicular Technology Conference, 2001. VTC 2001 Fall,* vol. 4, pp. 2623-2625, 2001.

[13] C. D. Bond, C. S. Guenzer and C. A. Carosella, "Intermodulation Generation by Electron Tunneling Through Aluminum-Oxide Films," *Proceedings of the IEEE,* vol. 67, no. 12, pp. 1643-1652, December 1979.

[14] P. O. Ho, W. S. Wilkinson and A. C. Tseung, "The Suppression of Intermodulation Product Generation in Materials and Structures used in Radio Communications," *IEE Colloquium on Passive Intermodulation Products in Antennas and Related Structures,* pp. 5/1-5/5, June 1989.

[15] J. Russer, "Phenomenological Modeling of Passive Intermodulation (PIM) due to Electron Tunneling at Metallic Contacts," *2006 IEEE MTT-S International Microwave Symposium Digest,* pp. 1129-1132, June 2006.

[16] J. Henrie, A. Christianson and W. J. Chappell, "Engineered Passive Nonlinearities for Broadband Passive Intermodulation Distortion Mitigation," *IEEE Microwave and Wireless Components Letters,* vol. 19, no. 10, pp. 614-616, September 2009.

[17] J. Henrie, A. Christianson and W. J. Chappell, "Prediction of Passive Intermodulation From Coaxial Connectors in Microwave Networks," *IEEE Transactions on Microwave Theory and Techniques,* vol. 56, no. 1, pp. 209-216, January 2008.

[18] A. W. Scott and R. Frobenius, RF Measurements for Cellular Phones and Wireless Data Systems, 1 ed., New Jersey: Wiley-IEEE Press, 2008, 503 p.

[19] IEC, "IEC 62037-1:2012," [Online]. Available: https://webstore.iec.ch/publication/6331. [Accessed 3 December 2015].

[20] Kaelus, "PIM FAQs," [Online]. Available: http://www.kaelus.com/en/services-and-support/faqs#collapse20k. [Accessed 3 December 2015].

[21] IEC, "TC 46/WG 6 Passive Intermodulation Measurement (PIM)," IEC, [Online]. Available: http://www.iec.ch/dyn/www/f?p=103:14:0::::FSP_ORG_ID,FSP_LANG_ID:2248,25. [Accessed 3 December 2015].

[22] V. Lehtinen, T. Lähteensuo, P. Vasenkari, A. Piipponen and M. Valkama, "Gatin Factor Analysis of Maximum Power Reduction in Multicluster LTE-A Uplink Transmission," *2013 IEEE Radio and Wireless Symposium (RWS),* pp. 151-153, January 2013.

[23] 3GPP, "ETSI TS 136 101 V12.9.0, LTE; Evolved Universal Terrestrial Radio Access (E-UTRA); User Equipment (UE) radio transmission and reception, 3GPP TS 36.101 V12.9.0 Release 12," October 2015. [Online]. Available: http://www.etsi.org/deliver/etsi_ts%5C136100_136199%5C136101%5C12.09.00_60%5Cts_136101v120900p.pdf. [Accessed 26 November 2015].

[24] H. Holma and A. Toskala, LTE Advanced: 3GPP Solution for IMT-Advanced, 1st ed., John Wiley & Sons, 2012, 249 p.

[25] M. Nohrborg, "LTE Overview," 3GPP, [Online]. Available: http://www.3gpp.org/technologies/keywords-acronyms/98-lte. [Accessed 16 November 2015].

[26] 3GPP, "Overview of 3GPP Release 8 V0.3.3," 2014.

[27] 3GPP, "Overview of 3GPP Release 10 V0.2.1," 2014.

[28] 3GPP, "Carrier Aggregation for LTE v.0.1.1," 2014.

[29] J. Wannstrom, "Carrier Aggregation explained," 3GPP, June 2013. [Online]. Available: http://www.3gpp.org/technologies/keywords-acronyms/101-carrier-aggregation-explained. [Accessed 16 November 2015].

[30] 3GPP, "TR 36.807 V10.0.0," Technical Report, 2012.

[31] 3GPP, "3GPP Work Items associated with Specification," 3GPP Spec 36.101, November 2015. [Online]. Available: http://www.3gpp.org/DynaReport/SpecVsWi--36101.htm. [Accessed 19 November 2015].

[32] 3GPP, "ETSI TS 136 104 V12.9.0, LTE; Evolved Universal Terrestrial Radio Access (E-UTRA); Base Station (BS) radio transmission and reception, 3GPP TS 36.104 V12.9.0 Release 12," October 2015. [Online]. Available: http://www.etsi.org/deliver/etsi_ts%5C136100_136199%5C136104%5C12.09.00_60%5Cts_136104v120900p.pdf. [Accessed 27 November 2015].

[33] ITU-R, "Recommendation ITU-R SM.329-10, Unwanted emissions in the

spurious domain," 2003.

[34] 3GPP, "ETSI TS 136 106 Technical Specification, LTE; E-UTRA; FDD repeater radio transmission and reception, 3GPP TS 36.106 V12.1.0 Release 12," February 2015. [Online]. Available: http://www.etsi.org/deliver/etsi_ts/136100_136199/136106/12.01.00_60/ts_136106v120100p.pdf. [Accessed 19 November 2015].

[35] 3GPP, "ETSI TR 136 912 V12.0.0 Technical Report, LTE; Feasibility study for Further Advancements for E-UTRA (LTE-Advanced), 3GPP TR 36.912 V12.0.0 Relese12," September 2014. [Online]. Available: http://www.etsi.org/deliver/etsi_tr%5C136900_136999%5C136912%5C12.00.00_60%5Ctr_136912v120000p.pdf. [Accessed 20 November 2015].

[36] C. S. Park, L. Sundsröm, A. Wallén and A. Khayrallah, "Carrier aggregation for LTE-advanced: design challenges of terminals," *IEEE Communications Magazine*, vol. 51, no. 12, pp. 76-84, December 2013.

[37] Multicomp, "BAT-54- Series, Datasheet V1.1," 5 October 2011. [Online]. Available: http://www.farnell.com/datasheets/1317753.pdf. [Accessed 1 February 2016].

[38] Bourns, "CHF2010xNP Series 10 W Power RF Chip Termination/Resistor, Datasheet," [Online]. Available: http://www.farnell.com/datasheets/1483747.pdf. [Accessed 23 February 2016].